Modelling the impact of climate variability on the effectiveness of seasonal indoor residual spraying

Alexis Martin-Makowka[1,2], James D. Munday[1,2], Adrian Mark Tompkins[3], Cyril Caminade[3], Nakul Chitnis[1,2]

1 Swiss Tropical and Public Health Institute, Allschwil, Switzerland
2 University of Basel, Basel, Switzerland
3 Earth System Physics, Abdus Salam International Centre for Theoretical Physics, Trieste, Italy

Abstract

Malaria transmission is strongly modulated by climate, yet most mechanistic models used for health policy evaluation do not explicitly account for climate-driven variability in mosquito dynamics. Here, we present a novel modelling framework that couples VECTRI, a climate-sensitive model for malaria, with OpenMalaria, a detailed individual-based model of malaria epidemiology and intervention impact. This integrated approach enables simulation of transmission processes that respond to interannual climate fluctuations while retaining the capacity to evaluate realistic intervention strategies.

We apply this framework to Mozambique, a high-burden country for malaria, with pronounced climatic seasonality and extensive routine surveillance data. Using district-level incidence time series from the ten highest-incidence districts, we validate the modelling framework and compare its performance with the standalone versions of VECTRI and OpenMalaria. The combined framework reproduces malaria seasonality more accurately than the two single models, with improved timing of incidence peaks in 7 out of 10 high-incidence districts and a closer representation of evolution of transmission throughout the season, as measured by the seasonality index, in 7 out of 10 districts.

We then use the coupled system to assess how climate-driven interannual variability affects the predicted effectiveness of indoor residual spraying, a key seasonal malaria control intervention in Mozambique. Integrating climate-driven interannual variability into OpenMalaria substantially impacts the modeled effectiveness of indoor residual spraying. The joint modelling framework increases the estimated protective effectiveness of indoor residual spraying in reducing incidence by up to 11% and delayed the optimal deployment window by two weeks.

Our results demonstrate that climate-informed mechanistic models can meaningfully alter estimates of intervention impact and improve the realism of malaria predictions. The joint OpenMalaria-VECTRI framework provides a flexible tool for national malaria programs seeking to evaluate seasonal interventions under varying climatic scenarios.

Author summary

Malaria transmission in Mozambique changes from year to year because mosquito populations strongly depend on rainfall and temperature. However, most models used to guide malaria control planning do not fully capture these climate-driven fluctuations. We developed a new modelling approach that links two existing tools: VECTRI, which simulates climate-sensitive mosquito and malaria dynamics, and OpenMalaria, which simulates malaria infections and the effects of interventions.

We validated this combined model using routine surveillance malaria data from Mozambique and found that it better captures observed seasonal and interannual patterns than standalone models. We then used it to explore how climate variability influences the effectiveness of indoor residual spraying, an important seasonal malaria control strategy. Accounting for climate-driven mosquito dynamics reduced the predicted protective effectiveness of indoor residual spraying by 11% and shifted the optimal deployment timing by approximately two weeks. These results show that integrating climate information into malaria models can improve the accuracy and usefulness of intervention planning.

Introduction

Malaria is one of the most consequential vector-borne infectious diseases worldwide, imposing a massive socio-economic and health burden on tropical and subtropical regions (WHO 2025). The disease is caused by protozoan parasites of the *Plasmodium* genus, transmitted to humans through the bites of infected female *Anopheles* mosquitoes (CDC 2024a; CDC 2024b). Despite the availability of effective treatments and well-established interventions, malaria continues to have a large health impact. After two decades of global progress, recent evidence points to a concerning stagnation — and in some settings a rebound — in malaria burden (WHO 2025). Multiple factors have contributed to this recent rebound, including growing insecticide and drug resistance. Increasing attention has also been drawn to the role of climate variability and extreme weather events in shaping malaria risk. The 2023 WHO World Malaria Report (WHO 2023) underlines the devastating impact of the 2022 floods in Pakistan, which led to an explosive malaria epidemic, with a five-fold increase in malaria cases reported in 2023.

Climate influences malaria transmission through several biological pathways. Temperature regulates mosquito development, survival, biting rate, and the speed of parasite replication within the mosquito (Mordecai et al. 2019). Rainfall controls the availability and persistence of larval habitats and food resources, thereby driving mosquito population dynamics (Thomson et al. 2017). As a consequence, mosquito population dynamics and by extension malaria transmission risk strongly respond to climatic variations (Reiner et al. 2015).

A broad arsenal of malaria prevention tools is available, including insecticide-treated nets, indoor residual spraying, chemoprevention strategies such as seasonal malaria chemoprevention, and more recently, malaria vaccines (Hemingway et al. 2016). Since the early 2000s, large-scale deployment of these interventions has contributed to substantial reductions in transmission and mortality (Bhatt et al. 2015). Many interventions are most effective when timed to coincide with peak transmission periods (Wagman et al. 2020; Cairns et al. 2012). In particular, indoor residual spraying — whose protective effect typically lasts three to six months (Sahu et al. 2020; Coleman et al. 2017). Aligning intervention timing with climatic drivers therefore remains a key challenge for national malaria control programs (NMCPs).

Mechanistic malaria models provide a valuable framework for understanding transmission processes and assessing intervention strategies. Existing models tend to prioritize different aspects of the system. VECTRI is a climate-driven malaria model that explicitly represents mosquito and parasite development as functions of temperature and rainfall, enabling detailed simulation of climate–transmission relationships (Tompkins and Ermert 2013)). OpenMalaria is a flexible individual-based model designed to evaluate a wide range of malaria interventions and their epidemiological effects in diverse settings (OpenMalaria 2026).

Several malaria transmission models incorporate climatic drivers to varying extents. The Liverpool Malaria Model explicitly represents the effects of temperature and precipitation on vector ecology and transmission dynamics, but it is primarily designed as a climate-driven transmission model and offers limited capacity for evaluating detailed intervention

scenarios (Ermert et al. 2011a; Ermert et al. 2011b; Hoshen and Morse 2004). EMOD provides a framework for modelling malaria interventions. It includes climate inputs, but its integration is not yet usable for detailed climate-impact assessments (P. Eckhoff 2013; P. A. Eckhoff 2012; P. A. Eckhoff 2011. Finally, malariasimulation is a lightweight, compartmental modelling framework in which climatic variables can modulate seasonal forcing or transmission intensity. However, climate effects are not represented mechanistically through explicit simulation of vector ecology or life stages (Charles et al. 2025). As a result, none of these models simultaneously offer a fully mechanistic representation of climate-driven vector dynamics together with a detailed and flexible framework for intervention effectiveness analysis.

In this study, we introduce a new approach that couples the strengths of existing malaria models, integrating VECTRI's representation of climate-sensitive entomological processes with OpenMalaria's capacity to simulate detailed intervention scenarios. This combined framework allows to examine how climate variability affects both malaria transmission and the impact of interventions. We apply this coupled modelling approach to Mozambique, a country with a persistently high malaria burden and a well-established relationship between climate and malaria incidence (Armando et al. 2025).

Malaria remains one of the greatest public health threats in Mozambique, with over 10 million cases reported annually since 2018 (Harp et al. 2021). It accounts for 29% of all deaths and 42% of deaths among children under five (Initiative 2023). Transmission intensity varies substantially between regions and between years, driven by climatic and socioeconomic factors. In Mozambique, *Anopheles funestus sensu stricto* is the dominant vector and *Plasmodium falciparum* is responsible for approximately 90% of all malaria cases (Máquina et al. 2024; Kloke et al. 2011; Aranda et al. 2005). Malaria transmission is highly seasonal, and varies across different regions in Mozambique, with the majority of cases occurring during the rainy season from November to April (Bertozzi-Villa et al. 2021; Ferrao et al. 2018). The analyses presented here thus provide insights relevant both for national malaria program planning and for broader climate–health modelling efforts.

A high-quality dataset from the National Malaria Control Program of Mozambique is available (Harp et al. 2021), enabling us to validate our framework for high-burden districts and assess the added value of integrating climate-driven and intervention-driven mechanistic models. This new framework allows us to incorporate climate-driven interannual variations in malaria transmission into a modelling tool designed for policy support (OpenMalaria), and we evaluate how accounting for these variations influences the predicted effectiveness of a standard seasonal intervention method: indoor residual spraying.

Methods

OpenMalaria

The two-model framework we describe in this paper is designed to account for interventions, with OpenMalaria responsible for capturing their effects. We use OpenMalaria version 47. OpenMalaria is a detailed individual-based stochastic simulation model designed to support malaria control policy by simulating *P. falciparum* transmission and the impact of interventions (OpenMalaria 2026; Chitnis et al. 2012; Smith et al. 2012; Smith et al. 2008). OpenMalaria consists of a human host module and a mosquito vector module that are interconnected. The human module simulates the within-host dynamics of malaria infections using an agent-based approach. When bitten by an infectious mosquito, a human host may become infected. The module tracks individual infection histories, including parasite densities, clinical symptoms, and the development of immunity over time. Host heterogeneity is represented explicitly, accounting for factors such as age, immunity status, and attractiveness to mosquitoes. The simulation proceeds in 5-day increments (pentads), updating each individual's infection status and immune profile. At each time step, the

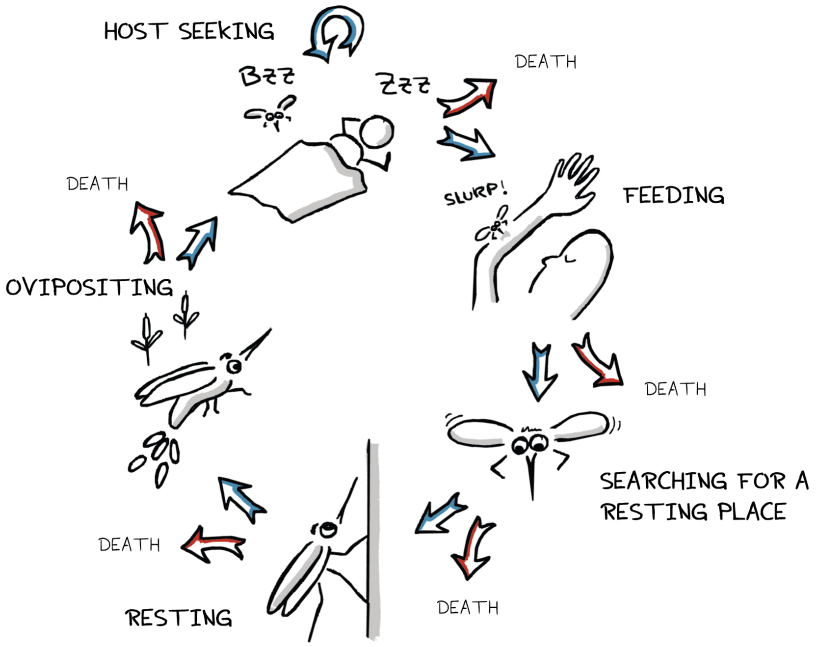

Figure 1: Gonotrophic cycle of *Anopheles spp.* mosquitoes. At each step of the gonotrophic cycle, female *anopheles* mosquitoes can either reach the next step or die, with some probability modeled by OpenMalaria.

model outputs which individuals are infected, allowing aggregation into population-level metrics such as malaria incidence and prevalence.

The mosquito module is a nested compartmental model updated daily. It tracks the number of blood-seeking female mosquitoes and their infection status: any infection status (including susceptible mosquitoes), infected or infectious, or infectious only. A blood-seeking female mosquito can find a host or die while doing so. Once a mosquito successfully finds a host, it initiates a gonotrophic cycle that involves blood feeding, resting and ovipositing, before a subsequent host-seeking. The probability of a mosquito successfully finding a host depends on host availability and species-specific feeding preferences. At each step of the gonotrophic cycle, mosquitoes face a risk of mortality. If a mosquito feeds on an infectious human, it becomes infected and undergoes a sporogonic cycle, after which it becomes infectious. The gonotrophic cycles of *Anopheles spp.* is described in Figure 1.

Simulations begin with a fully susceptible human population. Initially, only the human module is active, and malaria transmission is forced into the human population via an externally defined strictly seasonal entomological inoculation rate (EIR) time series. This period during which malaria is forced into the human population last lasts 90 years and allows for the buildup of immunity across a full generational turnover. After this period, the mosquito module is activated, and humans can now infect mosquitoes. The EIR is still guided by the input time series, and the model runs for an additional 30 years. During this phase, the emergence rate of mosquitoes is calibrated to ensure that the simulated EIR matches the input EIR. Once these two EIR time series are close enough, the input EIR can be removed, and the model proceeds autonomously with full vector-host dynamics for another 30-year burn-in period to stabilize malaria transmission. Following the burn-in period, interventions can be deployed to evaluate their effects on malaria transmission. OpenMalaria allows for parameter modifications representing diverse control measures, such as indoor residual spraying. Model outputs include the simulated EIR, clinical episode counts, and

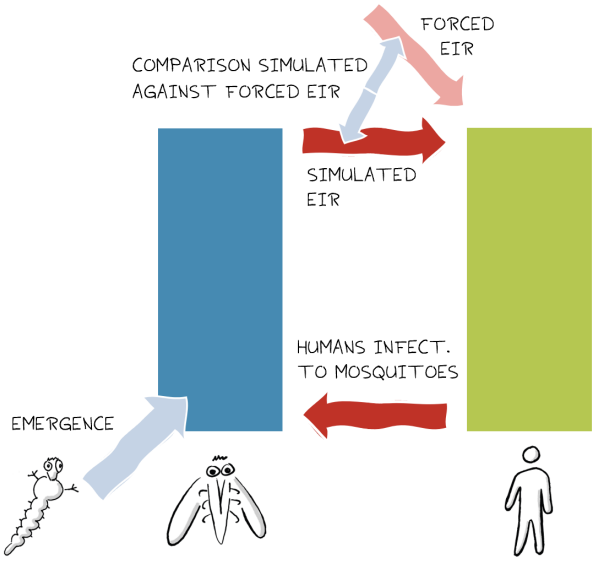

Figure 2: Overview of the human and mosquito modules of OpenMalaria and and their interaction. OpenMalaria consists of two interconnected modules: an individual-based human host module and a compartmental mosquito vector module. Initially, malaria transmission is forced using an external input entomological inoculation rate to allow immunity to build up in the human population. The mosquito module is then introduced, enabling full vector-host transmission dynamics. The system runs forward with or without interventions, which can be applied flexibly as parameter modifications.

infection prevalence. Importantly, OpenMalaria does not explicitly model climatic drivers of transmission. Instead, seasonal variations must be incorporated by prescribing seasonal input EIR accordingly. These variations will be reflected in the computed emergence rate. A detailed description of model mechanics is available in Chitnis et al. (2012), Smith et al. (2012), and Smith et al. (2008) and on the OpenMalaria GitHub repository (OpenMalaria 2026). Figure 2 summarizes how the human and mosquito modules interact.

VECTRI

The VECTRI model captures the effect of climate in the two-model framework. VECTRI (version 1.8.1) is a spatially explicit, climate-driven malaria model developed to simulate the impact of environmental factors on malaria dynamics at regional scales (Tompkins and Ermert 2013). Specifically designed for *An. gambiae* and *P. falciparum*, the model incorporates the effects of temperature, rainfall, and human population density on vector and parasite development. VECTRI operates on a grid-based spatial domain.

VECTRI simulates mosquito population dynamics through a bin-resolved compartmental structure representing the full aquatic and adult life stages. Larval development is influenced by water temperature and resource availability in breeding sites, which are modeled via a pond model forced by daily rainfall and air temperature data. Eggs laid by adult mosquitoes enter the larval stage and progress through successive bins, facing a probability of death or maturation to pupae. Once emerging as adults, mosquitoes initiate gonotrophic cycles that include host seeking, blood feeding, resting and egg laying. Each stage is temperature-dependent and subject to mortality rates. Transmission is modeled dynamically: mosquitoes may acquire infection upon biting an infectious human, initiating a sporogonic cycle that is also bin-resolved and sensitive to ambient temperature. Infectious mosquitoes, in turn, can transmit malaria to susceptible humans, triggering a within-host

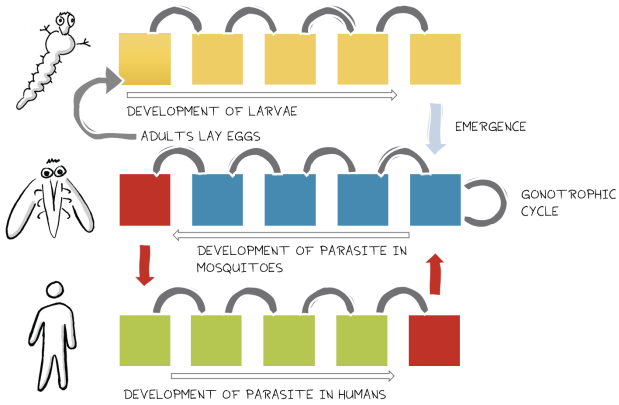

Figure 3: An overview of the VECTRI model. VECTRI is bin-resolved and models the progression of mosquito and parasite development, including larval growth, adult mosquito gonotrophic cycles, and parasite transmission dynamics within vectors and human hosts.

development period (sporogonic cycle). While mosquito parasite development is climate-dependent, human infection progression is modeled using a fixed developmental timeline.

VECTRI runs on a daily timestep and includes a one-year spin-up period, starting from an initial proportion of infected humans to allow the system to reach equilibrium. Outputs include key entomological indicators such as mosquito emergence rate, adult vector density, and the EIR, as well as epidemiological metrics like parasite prevalence and malaria case incidence. A schematic of the model components and transmission cycle is shown in Figure 3, and a detailed description is available in Tompkins (2024) and Tompkins and Ermert (2013).

Coupling of VECTRI with OpenMalaria

Our modeling framework integrates the climate-sensitive vector dynamics simulated by VECTRI into the transmission modeling environment of OpenMalaria. VECTRI simulations were conducted at a spatial resolution of $0.5° \times 0.5°$ (approximately 50km $\times$ 50km) across the African continent, using daily temperature and precipitation data from the CPC Global Unified Gauge-Based Analysis dataset for the period 1990–2023 (NOAA Physical Sciences Laboratory 2024). VECTRI also requires human population density data as input, here derived from the NASA's Gridded Population of the World, version 4 (GPWv4) from CIESIN (2018), available at 1km spatial resolution and interpolated to match the climate data grid. From the VECTRI output, we use the daily mosquito emergence rate as an input to OpenMalaria. The daily emergence rate is aggregated to match the pentad (5-day) resolution used in OpenMalaria. We additionally record the mean annual EIR from VECTRI.

OpenMalaria simulation parameters are taken from the standard XML schema 47 (OpenMalaria 2024). Namely, population size is 10,000. Simulated mosquitoes are all *An. gambiae*. The simulation, after initialization period, spans from January 1st, 2017 to August 31st, 2023.

OpenMalaria is initialized with a constant (flat) forced EIR. The transmission level is set up to 10% of VECTRI's mean annual EIR for the selected location, to account for the reduction of intensity resulting of unknown local interventions; the exact level of intensity at this stage is not crucial as we will recalibrate the malaria metrics later. During the burn-in period, the simulated EIR is still perennial and the mosquito emergence rate is kept

constant. To incorporate the influence of VECTRI's climate-driven mosquito dynamics, we adjust the mosquito emergence rate in OpenMalaria to follow the seasonal and interannual variability in the mosquito emergence rate simulated by VECTRI. This is implemented as a larval control intervention in OpenMalaria, where the constant emergence rate is modulated based on VECTRI's relative deviations from its mean. Since the two models differ in scale – VECTRI expresses emergence per unit area (spatial density), while OpenMalaria uses absolute mosquito counts – we apply a relative scaling approach: the OpenMalaria emergence rate is adjusted proportionally to VECTRI's deviation from its overall average. For example, if VECTRI's emergence rate at a given time is half its 2017-2023 average, the emergence rate in OpenMalaria is also halved.

Validation and comparison of modelling approaches

We validate the two-model framework using empirical malaria incidence data from Mozambique. Monthly counts of laboratory-confirmed malaria cases were obtained from the National Malaria Control Program (NMCP) (Harp et al. 2021). This data, reported through the *Boletín Epidemiológico Semanal*, covers the period from January 2017 to August 2023 and include all health facilities in 148 administrative districts. The fine spatial resolution of these aggregated data aligns well with the resolution of most global gridded climate observations. Per capita incidence values were computed using population estimates provided by the NMCP.

For this analysis, we focus on the ten districts with the highest mean malaria incidence during the study period (January 2017–August 2023). The geographic distribution of these districts is shown in Figure 4.

We ran simulations using three model configurations:

1. **The joint OpenMalaria and VECTRI framework**, as described in the previous section;
2. **VECTRI-only**, driven by the same climate and population density inputs as in the joint framework; and
3. **OpenMalaria-only**, using an average EIR equal to 10% of the EIR produced by VECTRI.

For the OpenMalaria-only setup, we imposed a seasonal pattern of transmission based on monthly average rainfall, following OpenMalaria's recommended approach. To account for the typical lag between rainfall and vector abundance, the rainfall-derived seasonality was shifted by one month. For the OpenMalaria-only and the the joint OpenMalaria-VECTRI framework, we replicated every simulation 100 times. For every output, we suppressed the outliers by removing the 5 highest and 5 lowest values, and calculated the mean of the remaining values.

Since the models produce outputs with different spatial and temporal units, we first harmonized the data before comparison. All simulated outputs were aggregated to a monthly resolution to match the temporal definition of the empirical data. We then rescaled model outputs to facilitate comparison, focusing on the timing, duration, and annual intensity of malaria transmission seasons rather than absolute values.

We extracted three main variables from the model outputs:

a) Entomological Inoculation Rate (EIR). For OpenMalaria and the joint framework, we used the variable *simulatedEIR*. For VECTRI-only simulations, we used *eir*. To ensure comparability, the VECTRI EIR was rescaled to match the mean EIR of the joint framework over the study period:

$$EIR^{*}_{VECTRI}(t) = \frac{\mu(EIR_{OpenMalaria+VECTRI})}{\mu(EIR_{VECTRI})} \cdot EIR_{VECTRI}(t), \tag{1}$$

where $\mu(\cdot)$ denotes the temporal mean over the simulation period.

b) Malaria incidence. Empirical incidence in cases per 10,000 people per month was obtained from the NMCP data. For OpenMalaria and the joint malaria modelling framework, we used the variable *nUncomp* (number of uncomplicated malaria episodes) as a proxy. We divided *nUncomp* by the simulated population: 10,000. For VECTRI, we used variable *cases*. Each malaria model's simulated incidence was rescaled so that its mean matched the mean empirical incidence over the study period, similarly to the EIR calculation described in equation 1.

c) Malaria prevalence. For OpenMalaria and the joint framework, prevalence was derived from the variable *nPatent* (number of patent infections), that we divided by 10,000 people simulated. For VECTRI we extracted variable *PRd*. To ensure consistency, OpenMalaria and joint-framework prevalence outputs were rescaled to match the mean prevalence simulated by VECTRI, similarly as shown in equation 1.

To quantitatively assess the performance of the aforementioned models, we applied several complementary statistical analyses. To evaluate the timing of malaria incidence peaks, we employed a wavelet-based phase analysis following a method from Martin-Makowka et al. (2025). Specifically, we computed the cross-wavelet transform between the modeled and observed incidence time series and extracted the phase difference at the dominant periodicity (that is, in our case the 12-month period). The phase difference corresponds to the peak-to-peak time offset between the two time series, and can be expressed in months. When the modeled and empirical series were positively correlated, this phase difference

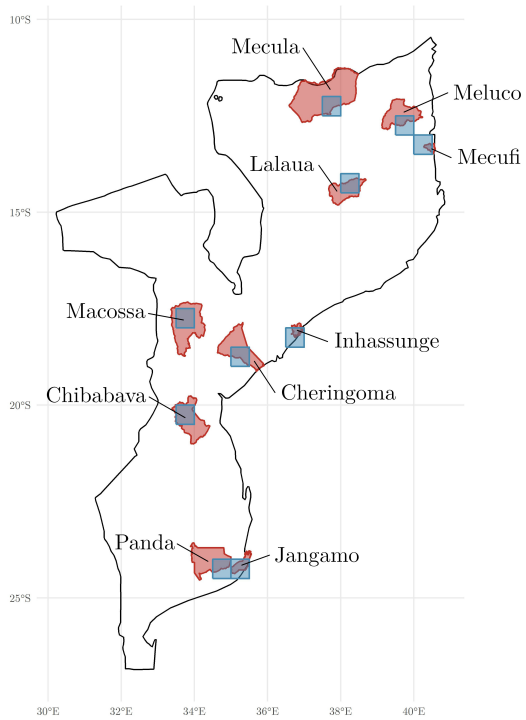

Figure 4: Map of the 10 districts in Mozambique with the highest incidence over the study period January 2017 – August 2023. In red are the districts, and in blue the VECTRI grid cells representing these districts for which we extracted the climatic factors and run the VECTRI model. We selected the grid cell corresponding to each district by identifying the cell containing the district centroid.

directly represented the lag. When negatively correlated, half of the period (i.e., 6 months) was added to obtain the effective lag.

To assess the models ability to capture the interannual variability in malaria incidence, we compared modeled and observed annual values for each district. For each model configuration, we plotted the observed annual incidence against the modeled annual incidence and fitted a simple linear regression. Model accuracy is evaluated by observing whether the 1:1 line lays within the regression's confidence interval. In addition, we computed the mean absolute error between observed and modeled annual incidence for each district and model, providing a quantitative measure of deviation to the observed empirical value for annual incidence.

We also evaluated the ability of the models to reproduce the duration of the malaria transmission season. We defined this duration as the number of months per year with incidence values greater than or equal to the mean annual incidence. For each model and district, we plotted empirical versus modeled durations and applied a linear regression, as aforementioned. Furthermore, we computed the coefficient of variation given by the standard deviation of monthly incidence, normalized by its mean, for each district and model/empirical data. This coefficient of variation served as a proxy for a seasonality index, quantifying the relative strength of intra-annual variation in malaria incidence.

Climate and effectiveness of indoor residual spraying

We examined how climate influences the timing and modeled effectiveness of seasonal control interventions. The aim of this analysis was to assess whether interannual climatic variations can substantially alter the predicted timing and impact of seasonal interventions. Here, we specifically focus on the interplay between climate and indoor residual spraying (IRS).

For this modeling experiment, we selected the district of Chibabava in Mozambique, identified as the district with the highest malaria incidence (9,810 cases per 10,000 people per year) during the period January 2017–August 2023. Local climate data was extracted for this district, and simulations were conducted assuming an annual EIR of approximately 28 infectious bites per person per year.

We first ran a standard OpenMalaria-only simulation in which the EIR seasonality was imposed following the rainfall seasonal pattern, shifted by one month. We iteratively repeated the simulations, deploying an IRS intervention once a year at time t (see below). The same set of simulations was then performed using the joint OpenMalaria-VECTRI modelling framework, with and without IRS deployment. For each simulation, we extracted the time series of simulated EIR (*simulatedEIR*), the number of uncomplicated malaria episodes (*nUncomp*), and the simulated malaria prevalence (*nPatent*).

When using identical input EIRs, minor discrepancies may arise between the simulated EIRs produced by the OpenMalaria-only and the joint OpenMalaria-VECTRI modelling framework due to nonlinear effects driven by interannual climate variations. To minimize such inconsistencies, we adjusted the input EIR for the joint model through an iterative, trial-and-error procedure to ensure comparable baseline transmission levels. In the absence of IRS, the adapted simulations produced mean EIRs of 28.087 and 27.559 infectious bites per person per year for the OpenMalaria-only and OpenMalaria-VECTRI framework, respectively.

IRS interventions were deployed annually at fixed times t, corresponding to either the 1st or 16th day of a given month. To avoid bias from the initial high-transmission period in early 2017 – which would disproportionately benefit earlier deployment schedules – the first IRS application was scheduled between July 1, 2017 and June 16, 2018. IRS intervention parameters followed the *IRS05* configuration described in Golumbeanu et al. (2024), which represents bendiocarb as the active ingredient tested against *An. gambiae* (Chitnis et al. 2010). The decay in insecticidal concentration was modeled using an exponential function

with a characteristic lifetime of $L = 0.17$ year and an initial postprandial killing effect of 0.81. The preprandial killing effect and deterrency were set to zero, and an IRS coverage of 90% was assumed. The intervention was deployed annually at the prescribed start times t.

The protective effect of IRS applied annually at time t was quantified relative to a no-intervention baseline. Protective factors were computed over the period from July 1st, 2017 to June 30th, 2023, for both transmission and disease outcomes: (i) the number of infectious bites averted, and (ii) the number of uncomplicated malaria episodes averted. The protective factor against malaria incidence was defined as:

$$\mathrm{PF}(t) = 1 - \frac{\mathrm{nUncomp}(\mathrm{IRS}(t))}{\mathrm{nUncomp}(\text{no intervention})}, \tag{2}$$

where, $\mathrm{nUncomp}(\mathrm{IRS}(t))$ represents the total number of uncomplicated malaria episodes in the simulation with IRS deployed at time t, and nUncomp(no intervention) represents the corresponding number without IRS. A similar computation was applied to EIR to estimate the protective factor against disease transmission.

Results

Empirical malaria incidence

We first examined the temporal evolution of empirical malaria incidence data from the NMCP in Mozambique. The spatial and temporal distribution of incidence for the ten districts with the highest malaria burden during the study period (January 2017–August 2023) is shown in Figure 5. These districts were selected because they collectively account for the majority of reported malaria cases nationwide.

The analysis reveals substantial spatial heterogeneity in malaria trends across Mozambique. Several districts located in the northern and southern regions (Mecula, Meluco, and Panda) exhibit a clear decreasing trend in annual malaria incidence over time. In contrast, smaller coastal districts such as Mecufi, Jangamo, and Ihhassunge show no consistent long-term trend but share a similar temporal pattern, with distinct incidence peaks observed in 2019, 2022, and 2023. The district of Lalaua, located in the central-northeastern region, shows an increase in malaria incidence around 2021 followed by a gradual decline toward the end of the study period. The two central-northern districts, Macossa and Cheringoma, both display bimodal patterns, with elevated incidence levels in 2019–2020 and again in 2023. The district of Chibabava in the center-south stands out as the area with the highest malaria incidence overall. It exhibits an upward trend in malaria incidence throughout the study period.

Model validation

We validated the performance of the OpenMalaria-only and VECTRI-only simulations, together with the joint OpenMalaria-VECTRI modelling framework. The modeled time series for the Chibabava district are presented in Figure 6, while results for the remaining districts are provided in the Appendix (Figures 10–12).

Figure 6a shows the evolution of the EIR across models, together with associated rainfall and VECTRI-simulated mosquito emergence rate, allowing us to relate transmission dynamics to climatic forcing. Rainfall in Chibabava is generally unimodal, with an austral summer rainy season lasting from December to March and peaking around January, although bimodal patterns are also observed in 2018, 2022, and 2023. Occasionally, isolated rainfall peaks can occur, such as in July 2018. Simulated mosquito emergence rate closely follows rainfall seasonal cycles, typically without lag, although in 2018, 2022, and 2023, a one-month lag is observed. In VECTRI-only simulations, the EIR peaks are delayed by one month with respect to the emergence rate peaks. In OpenMalaria-only simulations, EIR

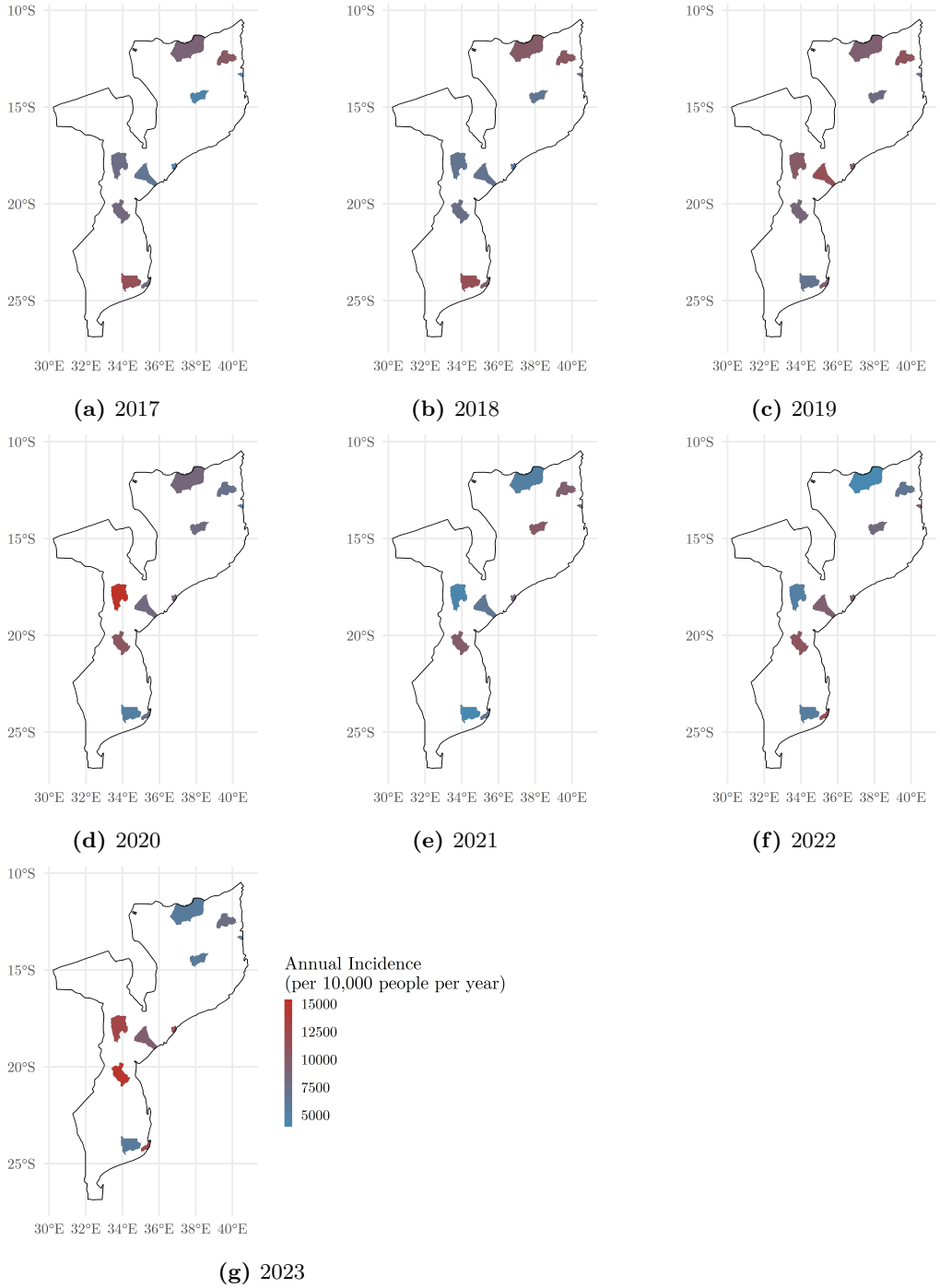

(a) 2017 **(b)** 2018 **(c)** 2019

(d) 2020 **(e)** 2021 **(f)** 2022

(g) 2023

Figure 5: Evolution of malaria incidence from 2017 to 2023, in the 10 districts bearing the highest incidence burden. The incidence is computed as the total number of confirmed malaria cases per 10,000 people and per year. The data for 2023 only ranges between January and August, and the annual incidence has been scaled by a corresponding factor.

patterns are highly regular: for years with a single rainfall peak, EIR closely aligns with the VECTRI peak, whereas for years with multiple rainfall peaks (2018, 2022, 2023), a single

EIR peak occurs, approximately representing an average of the rainfall peaks predicted by VECTRI. In the joint OpenMalaria-VECTRI framework, EIR peaks tend to coincide either with the VECTRI-only timing or occasionally occur one month later.

The modeled and empirical malaria incidence time series for Chibabava are compared in Figure 6b. The empirical data show an overall intensification of malaria transmission toward the end of the study period, with predominantly unimodal seasonal cycles peaking between March and May each year. Exceptions include a bimodal season in 2022, a moderate rebound during 2020–2021, and a small secondary increase in September 2018. The lag between VECTRI-simulated emergence and empirical incidence varies between 1 and 4 months, typically around 2 months. In general, VECTRI tends to lead the empirical signal by approximately two months, with simulated cases peaking concurrently with emergence rate, except in 2018, 2022, and 2023, where a one-month lag occurs. The OpenMalaria-only simulations show regular seasonal patterns with annual peaks around March, slightly ahead of the empirical data. These simulations reproduce the seasonal cycles but with weaker contrasts: the increase in incidence at the start of the season is more gradual, and the difference between high and low seasons is attenuated. The lag between emergence and incidence is again around two months. The joint OpenMalaria-VECTRI framework captures the onset of the transmission season well and follows the empirical timing more closely than standalone models, although it tends to lead slightly in 2018–2019. As for the other simulations, no clear long-term trend is observed. In such configuration, incidence typically peaks about two months after the simulated emergence rate peak.

Prevalence time series for Chibabava are shown in Figure 6c. No empirical prevalence data is available for direct comparison, and the analysis focuses on differences between models. VECTRI consistently predicts earlier peaks in prevalence than the other configurations, typically preceding the OpenMalaria-only peaks by about one month and the joint OpenMalaria-VECTRI framework by two months. Modeled prevalence fluctuates seasonally between roughly 40% and nearly 100%, depending on the year and model setup.

We further assessed the performance of the OpenMalaria-only, VECTRI-only, and joint OpenMalaria-VECTRI modelling framework using a suite of statistical analyses. Results for the Chibabava district are illustrated in Figure 7, while the corresponding analyses for the remaining districts are shown in the Appendix (Figures 13, 14, and 15).

We first quantified the timing accuracy of each model by estimating the lag between the modeled and empirical incidence time series using a wavelet-based phase-difference approach. This method captures the temporal evolution of lags across the study period and focuses on the dominant 12-month periodicity. Results for Chibabava are presented in Table 7a. For VECTRI, the modeled incidence leads the empirical signal by approximately five months at the beginning of the study period, decreasing monotonically to about four months by the end. The OpenMalaria-only model initially leads the empirical data by roughly two months, with the lag gradually reducing to slightly less than one month toward the end of the period. In contrast, the joint OpenMalaria-VECTRI configuration shows much smaller lags: it begins with a positive lag of about half a month (model slightly ahead), crosses zero (in synchrony) in early 2021, and ends with a negative lag of approximately -1 month, indicating a minor delay relative to observations.

We then compared the models' ability to reproduce annual incidence totals using scatter plots and linear regressions in Figure 7b. The VECTRI-only model shows large interannual variability, resulting in a wide confidence interval that does not include the 1:1 line. The OpenMalaria-only model exhibits almost no interannual variation: it predicts nearly identical incidence every year, yielding a very narrow and flat regression confidence interval with a slope near zero. In contrast, the joint OpenMalaria-VECTRI framework produces the steepest regression slope, and its confidence interval includes the 1:1 line, indicating that it better captures interannual changes in malaria incidence.

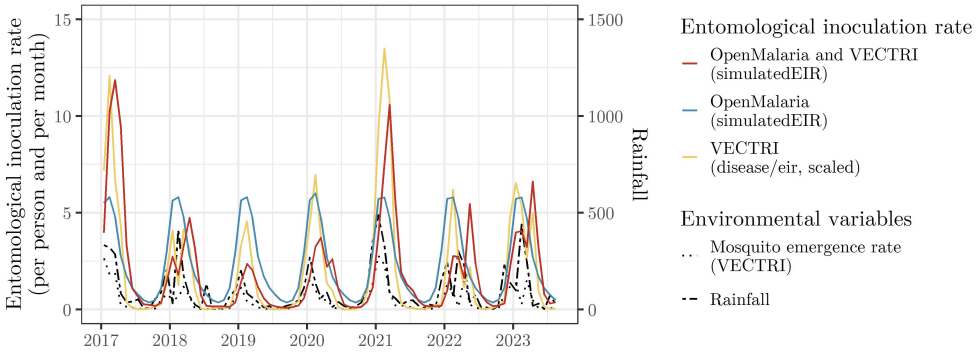

(a) Monthly entomological inoculation rate, as predicted by the different models. We multiplied the monthly entomological inoculation rate from VECTRI by a scaling coefficient to obtain the same mean between the VECTRI and the joint OpenMalaria-VECTRI framework.

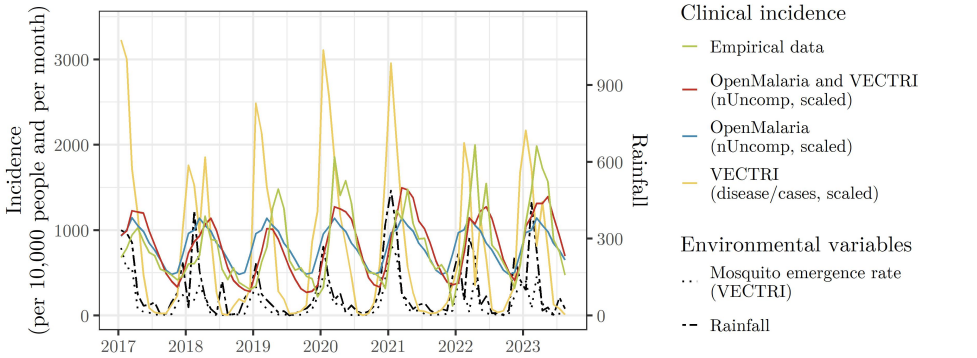

(b) Monthly malaria incidence, extracted from the empirical data or predicted by the different models. We multiplied each of the modeled incidence time series by a scaling coefficient, to obtain the same mean between all models and the empirical data.

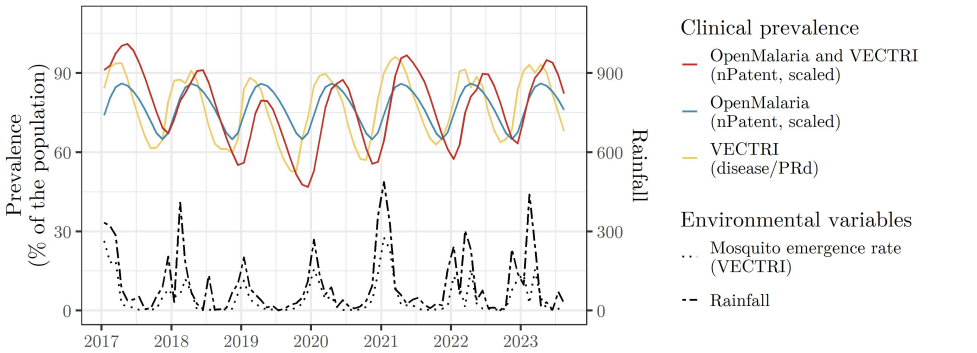

(c) Monthly malaria prevalence, as predicted by the different models. For both OpenMalaria and the joint OpenMalaria-VECTRI framework, we multiplied the prevalence time series by a scaling coefficient to obtain the same mean as in VECTRI.

Figure 6: Comparison between modeled or empirical malaria metrics for the district of Chibabava. Times series represent a) entomological inoculation rate, b) incidence, c) prevalence. The modeled time series have been extracted from VECTRI, OpenMalaria or the joint VECTRI–OpenMalaria framework. We additionally plotted the total monthly rainfall and the VECTRI-modeled emergence rate.

We also evaluated the ability of each model to reproduce the duration of the malaria transmission season. Duration was defined as the number of months per year with incidence greater than or equal to the annual mean (Figure 7c). For VECTRI, the regression between modeled and empirical duration has a negative slope, indicating that the model predicts shorter seasons in years with higher empirical incidence. The OpenMalaria-only model again produces nearly constant estimates each year, resulting in a flat slope and no meaningful confidence interval. The joint OpenMalaria-VECTRI framework displays substantial interannual dispersion, with simulated transmission seasons ranging from 3 to 8 months; however, its confidence interval includes almost the entire 1:1 line, indicating satisfactory agreement with empirical values.

Table 1 shows the mean lag (and its standard deviation) between modeled and empirical incidence for each district. For both VECTRI and OpenMalaria-only, all lags remain strictly positive, reflecting consistent anticipation of the empirical signal across districts. For each district, the model with lag closest to zero is highlighted in bold. Table 2 presents the mean absolute error (MAE) between observed annual incidence and the corresponding simulated annual values. The smallest MAE for each district is highlighted in bold. Finally, Table 3 shows the standard deviation of the monthly time series—used here as a seasonality index reflecting how strongly incidence fluctuates within each year. For each district, the simulated value closest to the empirical standard deviation is highlighted in bold.

district	VECTRI	OpenMalaria	OpenMalaria and VECTRI
Chibabava	4.85	1.81	**0.01**
Jangamo	4.01	**0.57**	-0.91
Meluco	6.65	4.74	**2.44**
Macossa	3.12	1.67	**-0.92**
Inhassunge	8.74	3.96	**2.43**
Cheringoma	4.51	1.75	**-0.31**
Panda	3.16	2.71	**1.24**
Lalaua	3.28	**0.61**	-1.16
Mecula	2.41	1.52	**-1.33**
Mecufi	3.11	**0.14**	-1.84

Table 1: Mean lags across models and districts, computed from the phase differences.

district	VECTRI	OpenMalaria	OpenMalaria and VECTRI
Chibabava	2205.61	1539.08	**1201.20**
Jangamo	2698.03	1540.85	**1302.14**
Meluco	1919.21	**1871.68**	1989.23
Macossa	**2891.25**	2970.39	3589.54
Inhassunge	2242.16	1704.17	**1548.63**
Cheringoma	1824.82	**1384.82**	1561.90
Panda	**1386.03**	2557.51	2825.62
Lalaua	2238.58	1702.31	**1488.39**
Mecula	**1995.09**	2351.82	2751.85
Mecufi	1736.88	1894.02	**1578.13**

Table 2: Mean absolute errors between the predicted and observed annual incidence, across models and districts.

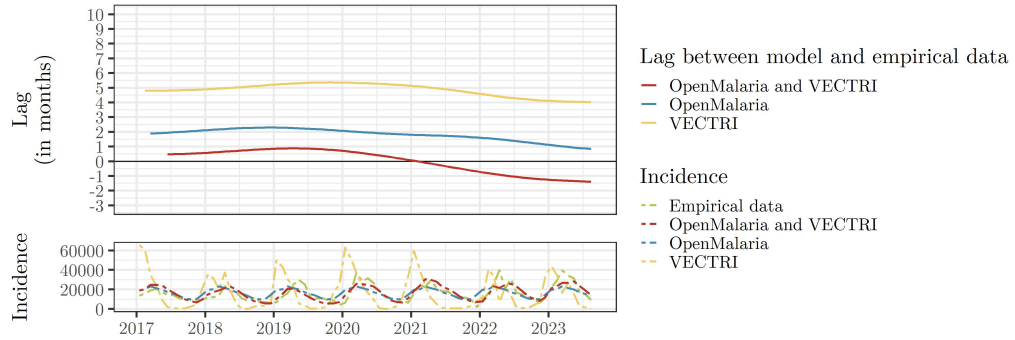

(a) Evolution of the lag between the modeled and the empirical incidence. A positive lag means that the model is ahead of the empirical data.

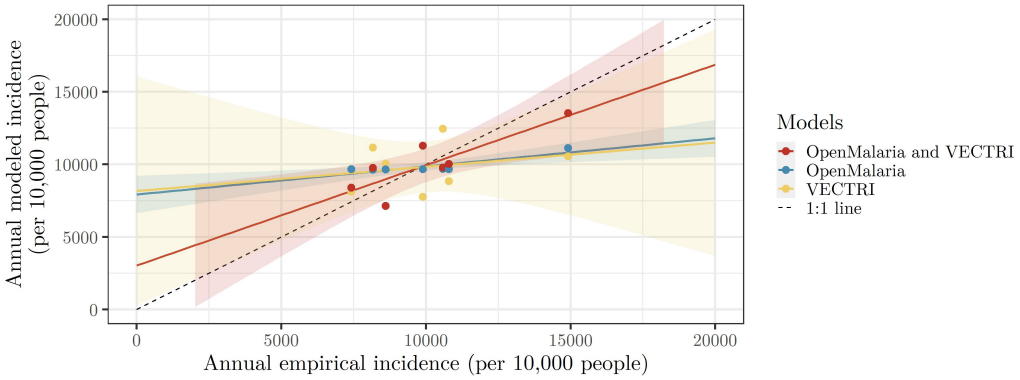

(b) Comparison of the empirical and modeled annual malaria incidence. For each model, we have scaled modeled incidence to have the same annual mean as the empirical incidence over the whole time period (i.e, we used the time series data from Figure 6b).

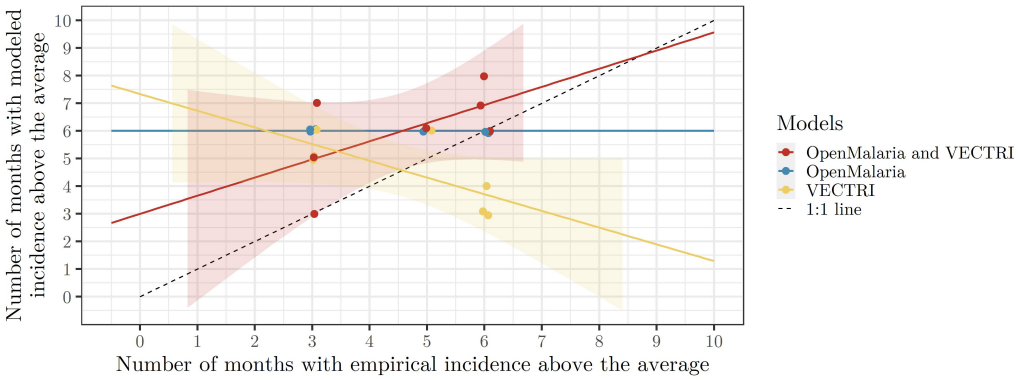

(c) Comparison of the annual number of months with malaria incidence above its average, empirical against predicted by the models.

Figure 7: Evaluation of the performance of the 3 different models (VECTRI, OpenMalaria and the joint *VECTRI–OpenMalaria* framework) in the district of Chibabava.

Impact of climate on the effectiveness of indoor residual spraying

Following validation of the joint OpenMalaria-VECTRI modelling framework, we now explore the simulated interplay between climate and malaria intervention dynamics. Figure 8

district	VECTRI	OpenMalaria	OpenMalaria and VECTRI	Empirical
Chibabava	1.08	0.27	**0.43**	0.53
Jangamo	0.85	0.19	**0.23**	0.34
Meluco	0.83	**0.39**	0.35	0.39
Macossa	1.23	0.41	**0.68**	0.76
Inhassunge	0.98	0.21	**0.27**	0.35
Cheringoma	1.06	0.25	**0.43**	0.52
Panda	0.92	0.18	**0.28**	0.52
Lalaua	0.87	0.48	**0.39**	0.38
Mecula	1.21	**0.51**	0.66	0.43
Mecufi	0.82	**0.37**	0.31	0.52

Table 3: Coefficients of variation of the modeled and empirical incidence time series normalized by mean, per district and model. Standard deviation is used as a proxy for seasonality index including the interannual variation (how well malaria transmissions seasons are marked).

presents the results for a scenario where IRS is deployed annually on November 16. The intervention produces a marked reduction in malaria transmission, reflected by a strong decrease in simulated EIR and prevalence. The reduction in malaria incidence is less pronounced but still noticeable. As expected, the concentration of active ingredients in the IRS intervention is highest immediately following deployment and declines rapidly thereafter, consistent with the exponential decay defined by the model parameterization.

In the OpenMalaria-only simulations, transmission patterns remain identical from year to year, since interannual variability is not explicitly represented. In contrast, the joint OpenMalaria-VECTRI modelling framework incorporates interannual fluctuations in climate, resulting in year-to-year variability in simulated EIR, incidence, and prevalence, even under identical intervention schedules.

Figure 9a summarizes the protective factor of IRS against EIR as a function of deployment timing and model. In the OpenMalaria-only simulations, IRS achieves an average protective factor of approximately 77.62%, corresponding to a 22.38% residual transmission relative to the non-intervention scenario. The optimal deployment timing in this case is December 1. In comparison, the joint OpenMalaria-VECTRI modelling framework predicts a stronger protective factor of 82.30%, reducing transmission to 17.70% of its original value. The maximum effectiveness is achieved when IRS is deployed on December 16 each year.

The protective factor against malaria incidence, representing the proportion of malaria episodes averted through IRS deployment, is shown in Figure 9b. The OpenMalaria-only model estimates an optimal deployment on December 1, yielding a protective factor of 20.28%. In contrast, the joint OpenMalaria-VECTRI simulations indicate that the most favorable deployment timing occurs around December 16, with a protective factor of 31.88%.

Discussion

In this study, we developed and evaluated a new malaria modelling framework that couples the climate-driven VECTRI model with the individual-based epidemiological model OpenMalaria. Our aim was to construct a modelling workflow capable of capturing interannual, climate-driven variability in malaria transmission while retaining the detailed representation of within-host dynamics and intervention effects implemented in OpenMalaria. We validated this framework using malaria incidence data from the highest-incidence districts in Mozambique. In addition, we assessed how interannual climatic variability influences the predicted effectiveness of seasonally-deployed indoor residual spraying (IRS).

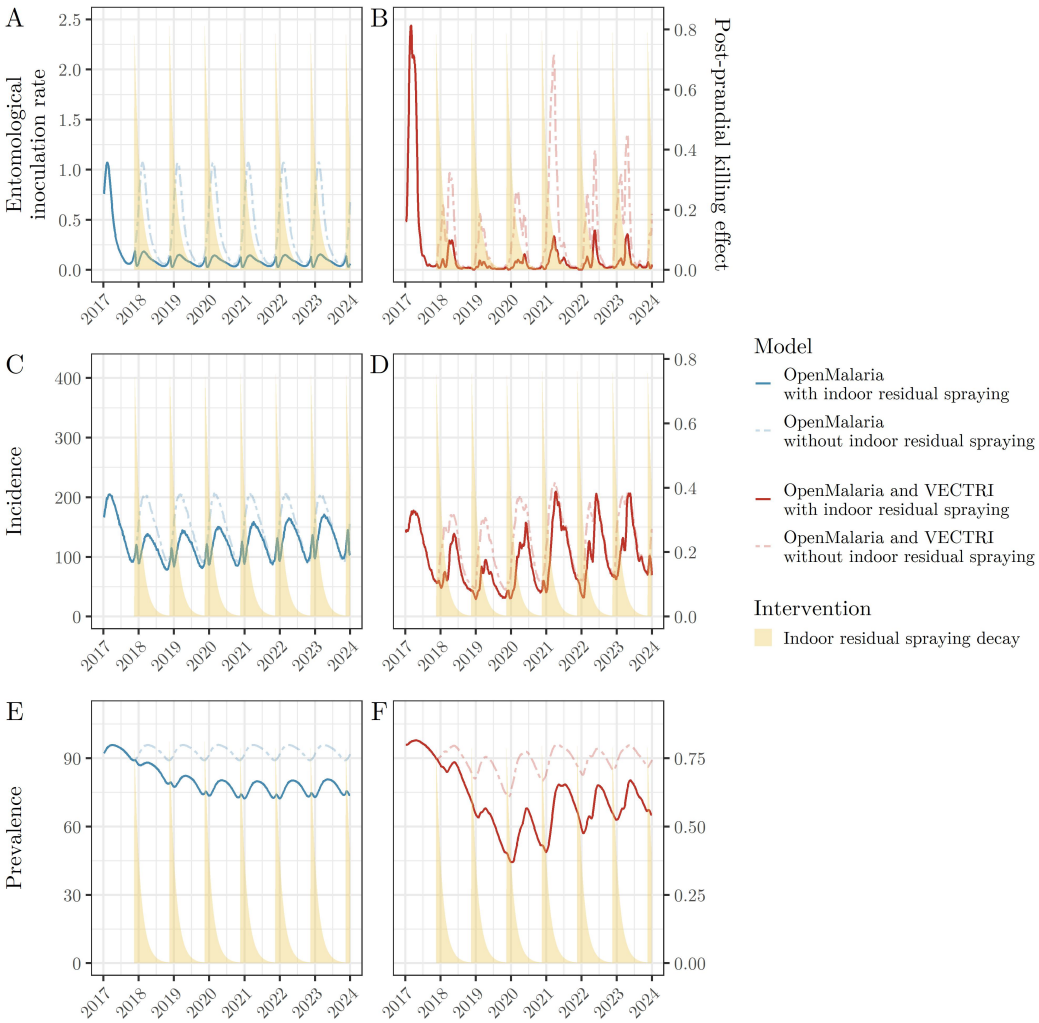

Figure 8: Simulated effect of the deployment of indoor residual spraying on different malaria metrics, using the standard version of OpenMalaria or the joint OpenMalaria-VECTRI framework. Indoor residual spraying is deployed every year on November 16. Study duration spans from January 2017 to December 2023. Plots A and B show the predicted effect of both models on the entomological inoculation rate (new infectious bites per person over the last 5 days), plots C and D on the incidence (new episodes in the last 5 days per 10,000 people), and plots E and F on the prevalence (% of the total population). Areas in yellow represent the deployment and decay of the post-prandial killing effect of the indoor residual spraying.

Malaria incidence in Mozambique has experienced pronounced trends and fluctuations over the past decade. Some of these variations likely reflect the timing and intensity of nationwide intervention campaigns. Mozambique deploys insecticide-treated nets in repeated mass distribution cycles – typically every three years – which can strongly influence interannual incidence patterns (Wetzler et al. 2022). At the same time, the country is highly exposed to extreme climatic events, including the impact of cyclones and floods. Mozambique was hit in 2017 by cyclone Dineo, in 2019 by cyclones Idai and Kenneth and in 2023 by cyclone Freddy (Rossi et al. 2024). These shocks are not always captured by monthly mean rainfall or temperature time series but can nevertheless disrupt malaria transmission

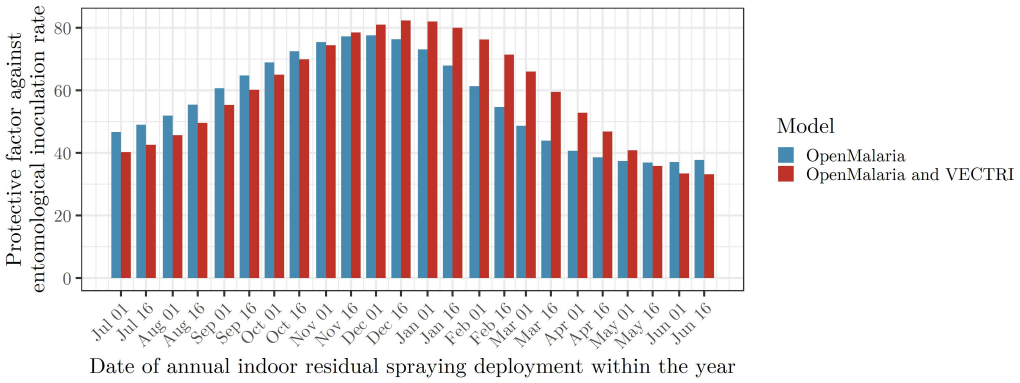

(a) Protective factor against entomological inoculation rate, in %. The protective factor assesses the percentage of averted malaria-infectious mosquito bites through the intervention at specific deployment timings.

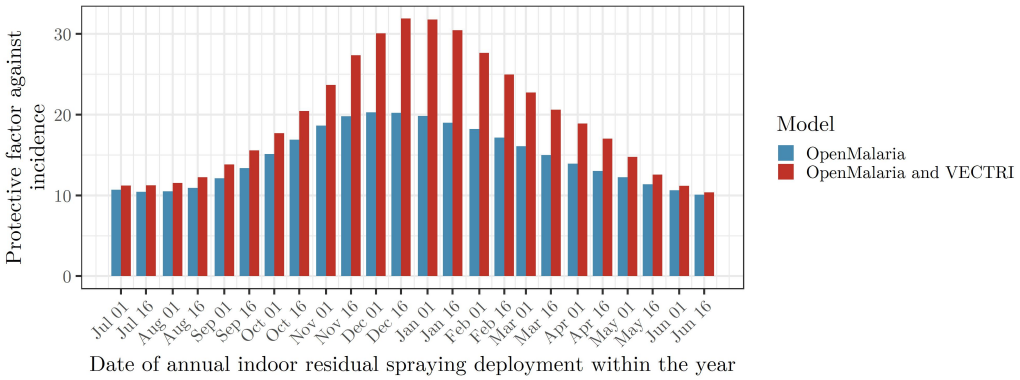

(b) Protective factor against incidence, in %. The protective factor assesses the percentage of averted malaria episodes through the intervention at specific deployment timings.

Figure 9: Protective factors of the indoor residual spraying interventions, depending on the selected model (standard OpenMalaria or the joint OpenMalaria and VECTRI modelling framework) and the date of the year when the indoor residual spraying intervention is deployed (Figure 8 is an example for indoor residual spraying deployment on November 16).

– or the reporting thereof. For instance, cyclone Freddy in 2023 caused extensive damages to health systems and may have altered malaria case detection, treatment availability, and human exposure patterns. Such climatic and non-climatic disturbances create complex incidence trends that can be challenging for mechanistic models to capture, especially when models are solely driven by rainfall and temperature data, as it is the case for our malaria modelling framework.

Validation in the district of Chibabava shows that the joint OpenMalaria-VECTRI framework accurately captures the timing of malaria incidence peaks. When extended to all districts, the combined model performs best in 7 out of 10 high-incidence districts, achieving average lags closest to zero. OpenMalaria-only performs slightly better in the remaining districts, suggesting that there is no universal "one-size-fits-all" model. Nonetheless, the overall improvement is substantial: while single models sometimes exhibit large timing errors, the combined model keeps average empirical–model lags below ∼2.5 months, even in districts where the models poorly perform. The districts with the largest remain-

ing discrepancies — Meluco, Inhassunge, and Mecúfi — share either weak seasonal rainfall regimes (Inhassunge) or strong rainfall seasonality but no consistent malaria seasonality (Meluco, Mecúfi). All three are coastal districts that may experience strong, irregular climatic shocks, including cyclones, flooding and surges. These events can influence mosquito ecology or health-facility reporting in ways that are not captured by rainfall and temperature data alone. Conversely, districts with clear rainfall seasonality, such as Chibabava, Macossa, Cheringoma, and Mecula, show highly accurate timing predictions under the joint modelling framework.

Observed lags between rainfall and malaria incidence in Mozambique and other African settings typically range from one to two months (Beloconi et al. 2023; Nyawanda et al. 2023; Ferrão et al. 2017), depending on rainfall intensity (Armando et al. 2023). A two-month lead time is generally considered optimal for early-warning systems (Armando et al. 2025). This reflects the cumulative time required for mosquito breeding, sporogony, and subsequent human infection (Reiner et al. 2015). Our combined model reproduces this characteristic lag structure: the occurrence of rainfall leads the malaria incidence peak by approximately two months.

Model performance on annual incidence values is less clear-cut. While the combined model performs well in Chibabava and outperforms single models in 5 out of 10 districts (notably in Macossa, Panda, and Mecula), prediction errors remain substantial (1,200–3,600 cases per 10,000 people). Both the joint and single models struggle to reproduce district-specific long-term trends, which may stem from temporal changes in intervention coverage, health-system functionality, socio-economic factors, or human mobility – factors not yet represented in the model.

The combined framework successfully captures the duration of the transmission season in Chibabava, with positive correlations between observed and simulated season lengths. Across districts, it also better reproduces the seasonality index – the standard deviation of monthly incidence – compared with single models, performing best in 7 out of 10 districts. These results align with the dominant role of rainfall and temperature in shaping malaria seasons (Reiner et al. 2015). By integrating climate-driven mosquito dynamics from VECTRI and accurate immunity profiles from OpenMalaria, the joint model effectively merges the strengths of both approaches.

Overall, the joint modelling framework shows clear improvements over single models, particularly for predicting timing and season duration, while improvements in intensity prediction remain more modest.

Because the combined model performs particularly well in highly seasonal, high-incidence settings such as Chibabava, it provides a meaningful basis for evaluating seasonal interventions such as IRS. In these simulations, IRS substantially reduced the entomological inoculation rate (EIR), consistent with its mode of action targeting indoor-resting, human-fed mosquitoes. The impact on incidence and prevalence is more modest: reductions in EIR also reduce population-level immunity, which dampens the downstream reduction in clinical cases. Under optimal deployment timing, OpenMalaria-only predicts EIR reductions of 77.62% and incidence reductions of 20.28%, whereas the combined model predicts larger effects – 82.30% and 31.88%, respectively.

Optimal IRS deployment is simulated in early December for OpenMalaria and mid-December for the combined framework. This difference reflects the improved representation of transmission season timing in the joint framework, further supporting the importance of integrating climate-driven variability. The inclusion of climate variables also enables the model to reproduce the near-absence of transmission during the dry season. In contrast, standard OpenMalaria assumes an idealized seasonal forcing with persistent low-level transmission risk year-round, which can dilute the predicted benefit of interventions. Thus, accounting for interannual climatic variation not only improves simulations but also yields different – and arguably more accurate – estimates of optimal intervention timing and expected effectiveness.

Several limitations remain. First, mosquito emergence in the current joint model is not directly affected by vector control interventions. In OpenMalaria, emergence is seasonally prescribed and independent of adult mosquito density, whereas in VECTRI it depends on larval dynamics and adult populations that directly rely on rainfall and temperature inputs. Ideally, the models should be dynamically coupled: OpenMalaria should pass intervention-induced mosquito mortality back to VECTRI, allowing VECTRI to adjust emergence rates dynamically. Implementing such two-way coupling is a priority for future work.

Second, although timing and seasonality are well captured, intensity predictions remain imperfect. However, evaluating the impact of seasonal intervention relies more strongly on an accurate representation of seasonality than on capturing the exact incidence values, since intervention efficacy is expressed relative to the same baseline model.

In conclusion, we have developed a novel modelling framework that merges climate-driven mosquito dynamics from VECTRI with the detailed human infection dynamics and intervention modelling of OpenMalaria. This combined approach captures interannual climate variability and improves predictions of malaria transmission timing and seasonality in high-incidence districts of Mozambique. When applied to seasonal interventions, our modelling framework reveals significant differences in the optimal deployment timing and impact of IRS compared to the standard OpenMalaria model, underscoring the importance of representing climate and interannual variability in malaria control assessments. The combined framework offers a promising platform for future analyses and for designing more context-specific malaria intervention strategies.

Acknowledgments

The authors thank Dr. Baltazar Candrinho, Director of the National Malaria Control Program of Mozambique, for the malaria incidence data used to validate the modelling framework. The authors also acknowledge Kevin Crowe, data analyst at The Washington Post, for facilitating access to these data.

A.M.M. and N.C. acknowledge support from the Gates Foundation [Grant number 025569 (A.M.M. and N.C.) and 081779 (N.C.)]

A.M.M., J.D.M., A.P.M., C.C., N.C. acknowledge support from the Wellcome Trust CLIMate SEnsitive DISease forecasting tool (CLIMSEDIS) research project [Grant number 225997/Z/22/Z].

References

Aranda, C., Aponte, J. J., Saute, F., Casimiro, S., Pinto, J., Sousa, C., Rosario, V. D., Petrarca, V., Dgedge, M., and Alonso, P. (Mar. 2005). "Entomological Characteristics of Malaria Transmission in Manhiça, a Rural Area in Southern Mozambique". In: *Journal of Medical Entomology* 42.2, pp. 180–186.

Armando, C. J., Rocklöv, J., Sidat, M., Tozan, Y., Mavume, A. F., Bunker, A., and Sewes, M. O. (June 2023). "Climate Variability, Socio-Economic Conditions and Vulnerability to Malaria Infections in Mozambique 2016–2018: A Spatial Temporal Analysis". In: *Frontiers in Public Health* 11, p. 1162535. ISSN: 2296-2565. DOI: 10.3389/fpubh.2023.1162535.

Armando, C. J., Rocklöv, J., Sidat, M., Tozan, Y., Mavume, A. F., and Sewe, M. O. (Apr. 2025). "Spatio-Temporal Modelling and Prediction of Malaria Incidence in Mozambique Using Climatic Indicators from 2001 to 2018". In: *Scientific Reports* 15.1, p. 11971. ISSN: 2045-2322. DOI: 10.1038/s41598-025-97072-6.

Beloconi, A., Nyawanda, B. O., Bigogo, G., Khagayi, S., Obor, D., Danquah, I., Kariuki, S., Munga, S., and Vounatsou, P. (May 2023). "Malaria, climate variability, and interventions: modelling transmission dynamics". In: *Scientific Reports* 13.1, p. 7367. ISSN: 2045-2322. DOI: 10.1038/s41598-023-33868-8.

Bertozzi-Villa, A., Bever, C. A., Koenker, H., Weiss, D. J., Vargas-Ruiz, C., Nandi, A. K., Gibson, H. S., Harris, J., Battle, K. E., Rumisha, S. F., Keddie, S., Amratia, P., Arambepola, R., Cameron, E., Chestnutt, E. G., Collins, E. L., Millar, J., Mishra, S., Rozier, J., Symons, T., Twohig, K. A., Hollingsworth, T. D., Gething, P. W., and Bhatt, S. (June 2021). "Maps and Metrics of Insecticide-Treated Net Access, Use, and Nets-per-Capita in Africa from 2000-2020". In: *Nature Communications* 12.1, p. 3589. ISSN: 2041-1723. DOI: 10.1038/s41467-021-23707-7.

Bhatt, S., Weiss, D. J., Cameron, E., Bisanzio, D., Mappin, B., Dalrymple, U., Battle, K. E., Moyes, C. L., Henry, A., Eckhoff, P. A., Wenger, E. A., Briët, O., Penny, M. A., Smith, T. A., Bennett, A., Yukich, J., Eisele, T. P., Griffin, J. T., Fergus, C. A., Lynch, M., Lindgren, F., Cohen, J. M., Murray, C. L. J., Smith, D. L., Hay, S. I., Cibulskis, R. E., and Gething, P. W. (Oct. 2015). "The effect of malaria control on Plasmodium falciparum in Africa between 2000 and 2015". In: *Nature* 526.7572, pp. 207–211. ISSN: 0028-0836, 1476-4687. DOI: 10.1038/nature15535.

Cairns, M., Roca-Feltrer, A., Garske, T., Wilson, A. L., Diallo, D., Milligan, P. J., Ghani, A. C., and Greenwood, B. M. (June 2012). "Estimating the potential public health impact of seasonal malaria chemoprevention in African children". In: *Nature Communications* 3.1, p. 881. ISSN: 2041-1723. DOI: 10.1038/ncomms1879.

Center for International Earth Science Information Network (CIESIN), C. U. (2018). *Gridded Population of the World, Version 4 (GPWv4): Population Count, Revision 11*. en. Project. Publisher: Earth Science Data Systems, NASA.

Centers for Disease Control and Prevention (2024a). *Life Cycle of Anopheles Mosquitoes*. Accessed: November 11, 2024.

— (2024b). *Malaria*. Accessed: November 11, 2024.

Charles, G., Winskill, P., Topazian, H., Challenger, J., Fitzjohn, R., Sheppard, R., Brewer, T., McCain, K., and Haile, L. (2025). *Malariasimulation: An Individual Based Model for Malaria*. Version R package version 2.0.2.

Chitnis, N., Hardy, D., and Smith, T. (May 2012). "A Periodically-Forced Mathematical Model for the Seasonal Dynamics of Malaria in Mosquitoes". In: *Bulletin of Mathematical Biology* 74.5, pp. 1098–1124. ISSN: 0092-8240, 1522-9602. DOI: 10.1007/s11538-011-9710-0.

Chitnis, N., Schapira, A., Smith, T., and Steketee, R. (Aug. 2010). "Comparing the Effectiveness of Malaria Vector-Control Interventions Through a Mathematical Model". In: *The American Society of Tropical Medicine and Hygiene* 83.2, pp. 230–240. ISSN: 0002-9637, 1476-1645. DOI: 10.4269/ajtmh.2010.09-0179.

Coleman, S., Dadzie, S. K., Seyoum, A., Yihdego, Y., Mumba, P., Dengela, D., Ricks, P., George, K., Fornadel, C., Szumlas, D., Psychas, P., Williams, J., Appawu, M. A., and Boakye, D. A. (Dec. 2017). "A reduction in malaria transmission intensity in Northern Ghana after 7 years of indoor residual spraying". In: *Malaria Journal* 16.1, p. 324. ISSN: 1475-2875. DOI: 10.1186/s12936-017-1971-0.

Eckhoff, P. (May 1, 2013). "Mathematical Models of Within-Host and Transmission Dynamics to Determine Effects of Malaria Interventions in a Variety of Transmission Settings". In: *The American Society of Tropical Medicine and Hygiene* 88.5, pp. 817–827. ISSN: 0002-9637, 1476-1645. DOI: 10.4269/ajtmh.12-0007.

Eckhoff, P. A. (Dec. 2011). "A Malaria Transmission-Directed Model of Mosquito Life Cycle and Ecology". In: *Malaria Journal* 10.1, p. 303. ISSN: 1475-2875. DOI: 10.1186/1475-2875-10-303.

Eckhoff, P. A. (Dec. 2012). "Malaria Parasite Diversity and Transmission Intensity Affect Development of Parasitological Immunity in a Mathematical Model". In: *Malaria Journal* 11.1, p. 419. ISSN: 1475-2875. DOI: 10.1186/1475-2875-11-419.

Ermert, V., Fink, A. H., Jones, A. E., and Morse, A. P. (Dec. 2011a). "Development of a New Version of the Liverpool Malaria Model. I. Refining the Parameter Settings and Mathematical Formulation of Basic Processes Based on a Literature Review". In: *Malaria Journal* 10.1, p. 35. ISSN: 1475-2875. DOI: 10.1186/1475-2875-10-35.

— (Dec. 2011b). "Development of a New Version of the Liverpool Malaria Model. II. Calibration and Validation for West Africa". In: *Malaria Journal* 10.1, p. 62. ISSN: 1475-2875. DOI: 10.1186/1475-2875-10-62.

Ferrao, J. L., Niquisse, S., Mendes, J. M., and Painho, M. (Apr. 2018). "Mapping and Modelling Malaria Risk Areas Using Climate, Socio-Demographic and Clinical Variables in Chimoio, Mozambique". In: *International Journal of Environmental Research and Public Health* 15.4, p. 795. ISSN: 1660-4601. DOI: 10.3390/ijerph15040795.

Ferrão, J. L., Mendes, J. M., and Painho, M. (Dec. 2017). "Modelling the Influence of Climate on Malaria Occurrence in Chimoio Municipality, Mozambique". In: *Parasites & Vectors* 10.1, p. 260. ISSN: 1756-3305. DOI: 10.1186/s13071-017-2205-6.

Golumbeanu, M., Briët, O., Champagne, C., Lemant, J., Winkel, M., Zogo, B., Gerhards, M., Sinka, M., Chitnis, N., Penny, M., Pothin, E., and Smith, T. (Sept. 2024). "AnophelesModel: An R Package to Interface Mosquito Bionomics, Human Exposure and Intervention Effects with Models of Malaria Intervention Impact". In: *PLOS Computational Biology* 20.9. Ed. by T. Bollenbach, e1011609. ISSN: 1553-7358. DOI: 10.1371/journal.pcbi.1011609.

Harp, R. D., Colborn, J. M., Candrinho, B., Colborn, K. L., Zhang, L., and Karnauskas, K. B. (Feb. 2021). "Interannual Climate Variability and Malaria in Mozambique". In: *GeoHealth* 5.2, e2020GH000322. ISSN: 2471-1403, 2471-1403. DOI: 10.1029/2020GH000322.

Hemingway, J., Shretta, R., Wells, T. N. C., Bell, D., Djimdé, A. A., Achee, N., and Qi, G. (Mar. 2, 2016). "Tools and Strategies for Malaria Control and Elimination: What Do We Need to Achieve a Grand Convergence in Malaria?" In: *PLOS Biology* 14.3, e1002380. ISSN: 1545-7885. DOI: 10.1371/journal.pbio.1002380.

Hoshen, M. B. and Morse, A. P. (Sept. 6, 2004). "A Weather-Driven Model of Malaria Transmission". In: *Malaria Journal* 3.1, p. 32. ISSN: 14752875. DOI: 10.1186/1475-2875-3-32.

Initiative, P. M. (Aug. 2023). *Mozambique Malaria Profile*. Tech. rep. PMI.

Kloke, R. G., Nhamahanga, E., Hunt, R. H., and Coetzee, M. (Dec. 2011). "Vectorial Status and Insecticide Resistance of Anopheles Funestus from a Sugar Estate in Southern Mozambique". In: *Parasites & Vectors* 4.1, p. 16. ISSN: 1756-3305. DOI: 10.1186/1756-3305-4-16.

Máquina, M., Opiyo, M. A., Cuamba, N., Marrenjo, D., Rodrigues, M., Armando, S., Nhate, S., Luis, F., Saúte, F., Candrinho, B., Lobo, N. F., and Paaijmans, K. P. (Jan. 2024). "Multiple Anopheles Species Complicate Downstream Analysis and Decision-Making in a Malaria Pre-Elimination Area in Southern Mozambique". In: *Malaria Journal* 23.1, p. 23. ISSN: 1475-2875. DOI: 10.1186/s12936-024-04842-0.

Martin-Makowka, A., Nyawanda, B. O., Beloconi, A., Bigogo, G., Khagayi, S., Munga, S., Munywoki, P. K., Danquah, I., Utzinger, J., and Vounatsou, P. (Mar. 2025). "Variation of Malaria Dynamics and Its Relationship to Climate in Western Kenya during 2008-2019: A Wavelet Approach". In: *eLife Sciences Publications, Ltd* 14.RP103597. DOI: 10.7554/elife.103597.1.

Mordecai, E. A., Caldwell, J. M., Grossman, M. K., Lippi, C. A., Johnson, L. R., Neira, M., Rohr, J. R., Ryan, S. J., Savage, V., Shocket, M. S., Sippy, R., Ibarra, A. M. S., Thomas, M. B., and Villena, O. (2019). "Thermal biology of mosquito-borne disease". In: *Ecology Letters* 22.10, pp. 1690–1708. ISSN: 1461-0248. DOI: 10.1111/ele.13335.

NOAA Physical Sciences Laboratory (2024). *CPC Global Unified Gauge-Based Analysis of Daily Precipitation and Temperature Data*. Accessed: December 20, 2024.

Nyawanda, B. O., Beloconi, A., Khagayi, S., Bigogo, G., Obor, D., Otieno, N. A., Lange, S., Franke, J., Sauerborn, R., Utzinger, J., Kariuki, S., Munga, S., and Vounatsou, P. (May 2023). "The relative effect of climate variability on malaria incidence after scale-up of interventions in western Kenya: a time-series analysis of monthly incidence data from 2008 to 2019". In: *Parasite Epidemiology and Control* 21, e00297. ISSN: 24056731. DOI: 10.1016/j.parepi.2023.e00297.

OpenMalaria (July 12, 2024). *OpenMalaria Example Scenario Schema 47*. GitHub. URL: https://github.com/SwissTPH/openmalaria/blob/schema-47.0/util/example/example_scenario.xml (visited on 10/23/2025).

— (2026). *An Open-Source C++ Program for Simulating Malaria Epidemiology and the Impacts on That Epidemiology of Interventions against Malaria*. Version 47. Swiss Tropical and Public Health Institute.

Reiner, R. C., Geary, M., Atkinson, P. M., Smith, D. L., and Gething, P. W. (Dec. 2015). "Seasonality of *Plasmodium falciparum* transmission: a systematic review". In: *Malaria Journal* 14.1, p. 343. ISSN: 1475-2875. DOI: 10.1186/s12936-015-0849-2.

Rossi, B., Formenti, B., Cerini, C., Tique, N., Da Celma Cossa, R., Boniotti, F., Comini, B., Tomasoni, L. R., and Castelli, F. (Feb. 2024). "Addressing Health Care Disruption in Rural Mozambique Due to Extreme Climate Events: Mobile Units Tackling Cyclones, Vaccine-Preventable Diseases, and Beyond". In: *Frontiers in Tropical Diseases* 5, p. 1328926. ISSN: 2673-7515. DOI: 10.3389/fitd.2024.1328926.

Sahu, S. S., Thankachy, S., Dash, S., Nallan, K., Swaminathan, S., Kasinathan, G., and Purushothaman, J. (Dec. 2020). "Evaluation of long-lasting indoor residual spraying of deltamethrin 62.5 SC-PE against malaria vectors in India". In: *Malaria Journal* 19.1, p. 19. ISSN: 1475-2875. DOI: 10.1186/s12936-020-3112-4.

Smith, T., Maire, N., Ross, A., Penny, M., Chitnis, N., Schapira, A., Studer, A., Genton, B., Lengeler, C., Tediosi, F., De Savigny, D., and Tanner, M. (Nov. 2008). "Towards a comprehensive simulation model of malaria epidemiology and control". In: *Parasitology* 135.13, pp. 1507–1516. ISSN: 0031-1820, 1469-8161. DOI: 10.1017/S0031182008000371.

Smith, T., Ross, A., Maire, N., Chitnis, N., Studer, A., Hardy, D., Brooks, A., Penny, M., and Tanner, M. (Jan. 2012). "Ensemble Modeling of the Likely Public Health Impact of a Pre-Erythrocytic Malaria Vaccine". In: *PLoS Medicine* 9.1. Ed. by S. Krishna, e1001157. ISSN: 1549-1676. DOI: 10.1371/journal.pmed.1001157.

Thomson, M. C., Ukawuba, I., Hershey, C. L., Bennett, A., Ceccato, P., Lyon, B., and Dinku, T. (Sept. 2017). "Using rainfall and temperature data in the evaluation of national malaria control programs in Africa". In: *American Journal of Tropical Medicine and Hygiene* 97.3_Suppl, pp. 32–45. ISSN: 0002-9637, 1476-1645. DOI: 10.4269/ajtmh.16-0696.

Tompkins, A. M. and Ermert, V. (Dec. 2013). "A regional-scale, high resolution dynamical malaria model that accounts for population density, climate and surface hydrology". In: *Malaria Journal* 12.1, p. 65. ISSN: 1475-2875. DOI: 10.1186/1475-2875-12-65.

Tompkins, A. M. (2024). *VECTRI Documentation*. Version v1.11.1.

Wagman, J., Cissé, I., Kone, D., Fomba, S., Eckert, E., Mihigo, J., Bankineza, E., Bah, M., Diallo, D., Gogue, C., Tynuv, K., Saibu, A., Richardson, J. H., Fornadel, C., Slutsker, L., and Robertson, M. (Dec. 2020). "Rapid reduction of malaria transmission following the introduction of indoor residual spraying in previously unsprayed districts: an observational analysis of Mopti Region, Mali, in 2017". In: *Malaria Journal* 19.1, p. 340. ISSN: 1475-2875. DOI: 10.1186/s12936-020-03414-2.

Wetzler, E. A., Park, C., Arroz, J. A. H., Chande, M., Mussambala, F., and Candrinho, B. (Apr. 2022). "Impact of Mass Distribution of Insecticide-Treated Nets in Mozambique, 2012 to 2025: Estimates of Child Lives Saved Using the Lives Saved Tool". In: *PLOS*

Global Public Health 2.4. Ed. by D. A. M. Villela, e0000248. ISSN: 2767-3375. DOI: 10.1371/journal.pgph.0000248.

WHO (2025). *World Malaria Report 2025: Addressing the Threat of Antimalarial Drug Resistance*. Geneva: World Health Organization, p. 213.

World Health Organization (2023). *World malaria report 2023*. ISBN: 978-92-4-008617-3. Geneva.

Appendix

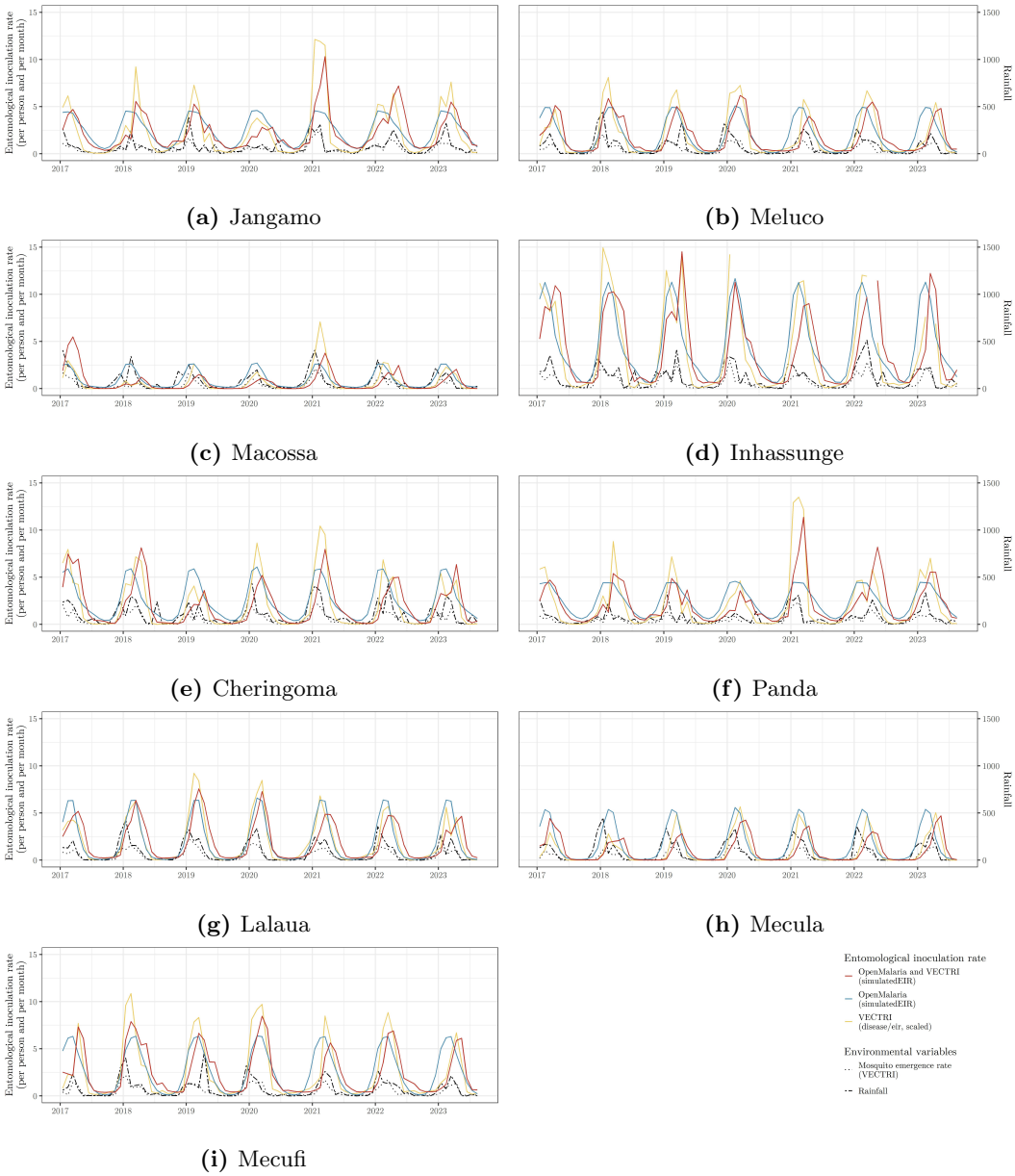

Figure 10: Monthly entomological inoculation rate, as predicted by the different models, for the 9 Mozambican districts with the highest incidence after Chibabava (shown in the main article). We transformed the variables 'simulatedEIR' (OpenMalaria, and OpenMalaria and VECTRI) and 'disease/eir' (VECTRI) into a monthly entomological inoculation rate. We multiplied the monthly entomological inoculation rate from VECTRI by a scaling coefficient to obtain the same mean between the VECTRI and the OpenMalaria and VECTRI models. We plotted the total monthly rainfall to display the rainy seasons. We plotted the VECTRI-modeled emergence rate to show the intermediate step in both the VECTRI and the joint OpenMalaria and VECTRI model.

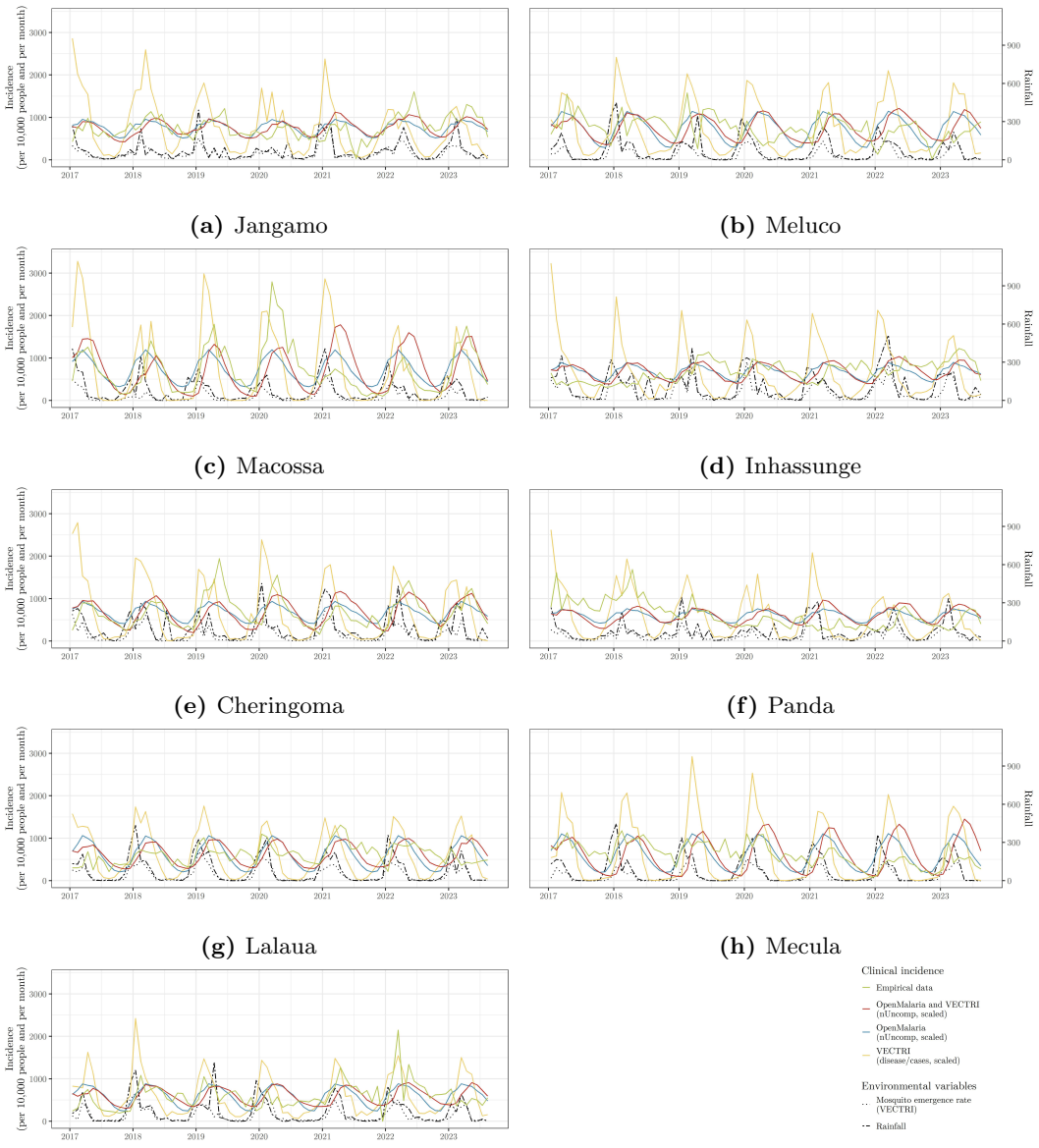

(a) Jangamo **(b)** Meluco **(c)** Macossa **(d)** Inhassunge **(e)** Cheringoma **(f)** Panda **(g)** Lalaua **(h)** Mecula **(i)** Mecufi

Figure 11: Monthly malaria incidence, extracted from the empirical data or predicted by the different models, for the 9 Mozambican districts with the highest incidence after Chibabava (shown in the main article). We transformed the variables 'nUncomp' (OpenMalaria, and OpenMalaria and VECTRI) and 'disease/cases' (VECTRI) into a monthly incidence. We multiplied each of the modeled incidence time series by a scaling coefficient, to obtain the same mean between all models and the empirical data. We plotted the total monthly rainfall to display the rainy seasons. We plotted the VECTRI-modeled emergence rate to show the intermediate step in both the VECTRI and the joint OpenMalaria and VECTRI model.

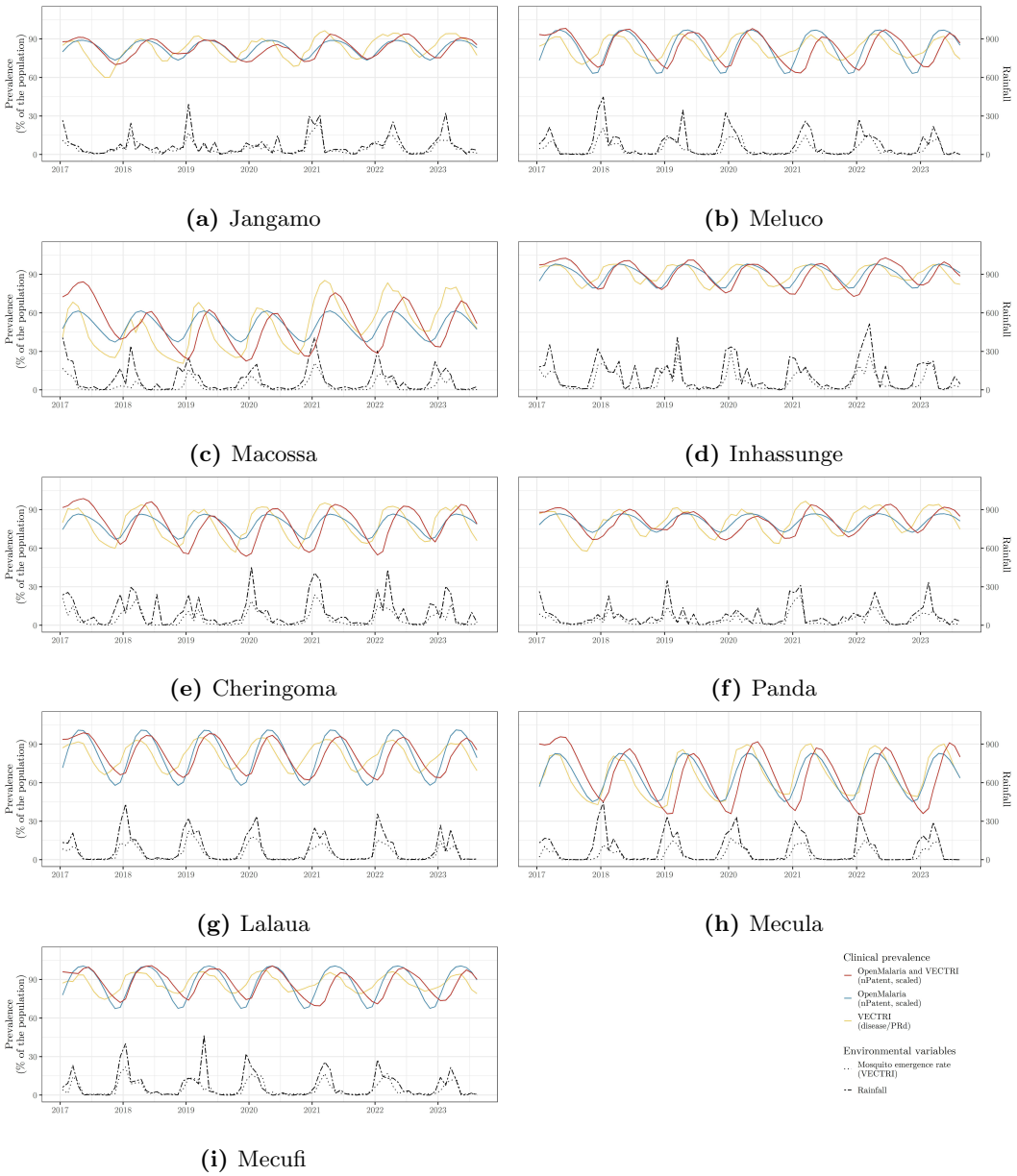

(a) Jangamo **(b)** Meluco **(c)** Macossa **(d)** Inhassunge **(e)** Cheringoma **(f)** Panda **(g)** Lalaua **(h)** Mecula **(i)** Mecufi

Figure 12: Monthly malaria prevalence, as predicted by the different models, for the 9 Mozambican districts with the highest incidence after Chibabava (shown in the main article). We transformed the variables 'nPatent' (OpenMalaria, and OpenMalaria and VECTRI) and 'disease/PRd' (VECTRI) into a monthly prevalence. For each of the OpenMalaria and the OpenMalaria and VECTRI models, we multiplied the prevalence time series by a scaling coefficient to obtain the same mean between the 3 models. We plotted the total monthly rainfall to display the rainy seasons. We plotted the VECTRI-modeled emergence rate to show the intermediate step in both the VECTRI and the joint OpenMalaria and VECTRI model.

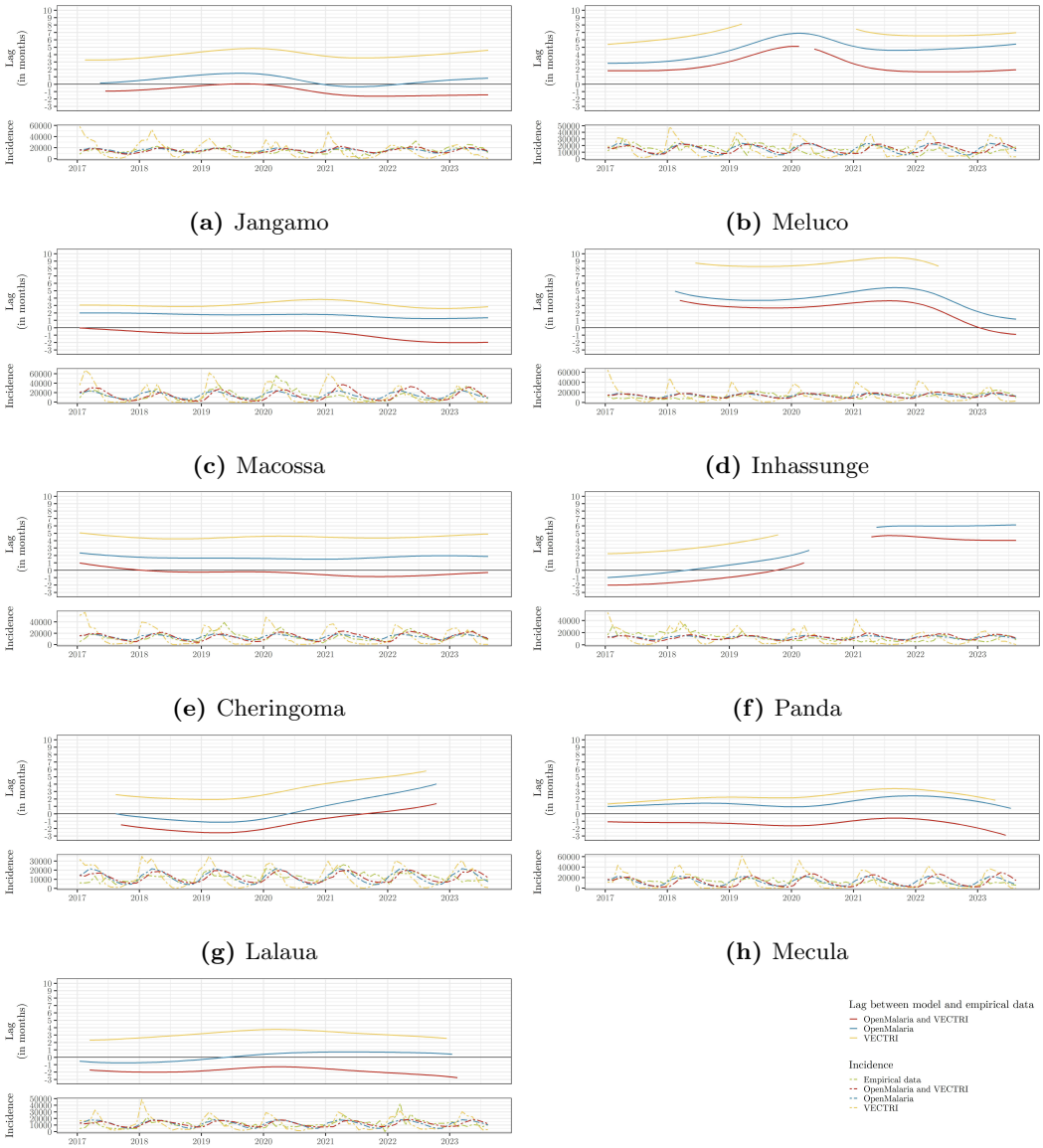

(a) Jangamo **(b)** Meluco **(c)** Macossa **(d)** Inhassunge **(e)** Cheringoma **(f)** Panda **(g)** Lalaua **(h)** Mecula **(i)** Mecufi

Figure 13: Evolution of the lag between the modeled and the empirical incidence, for the 9 Mozambican districts with the highest incidence after Chibabava (shown in the main article). Lags were obtained through the computation of the phase differences between each model and the empirical data. A positive lag means that the model is ahead of the empirical data. The incidence at the bottom is displayed for reference, and units are per 10,000 people per month.

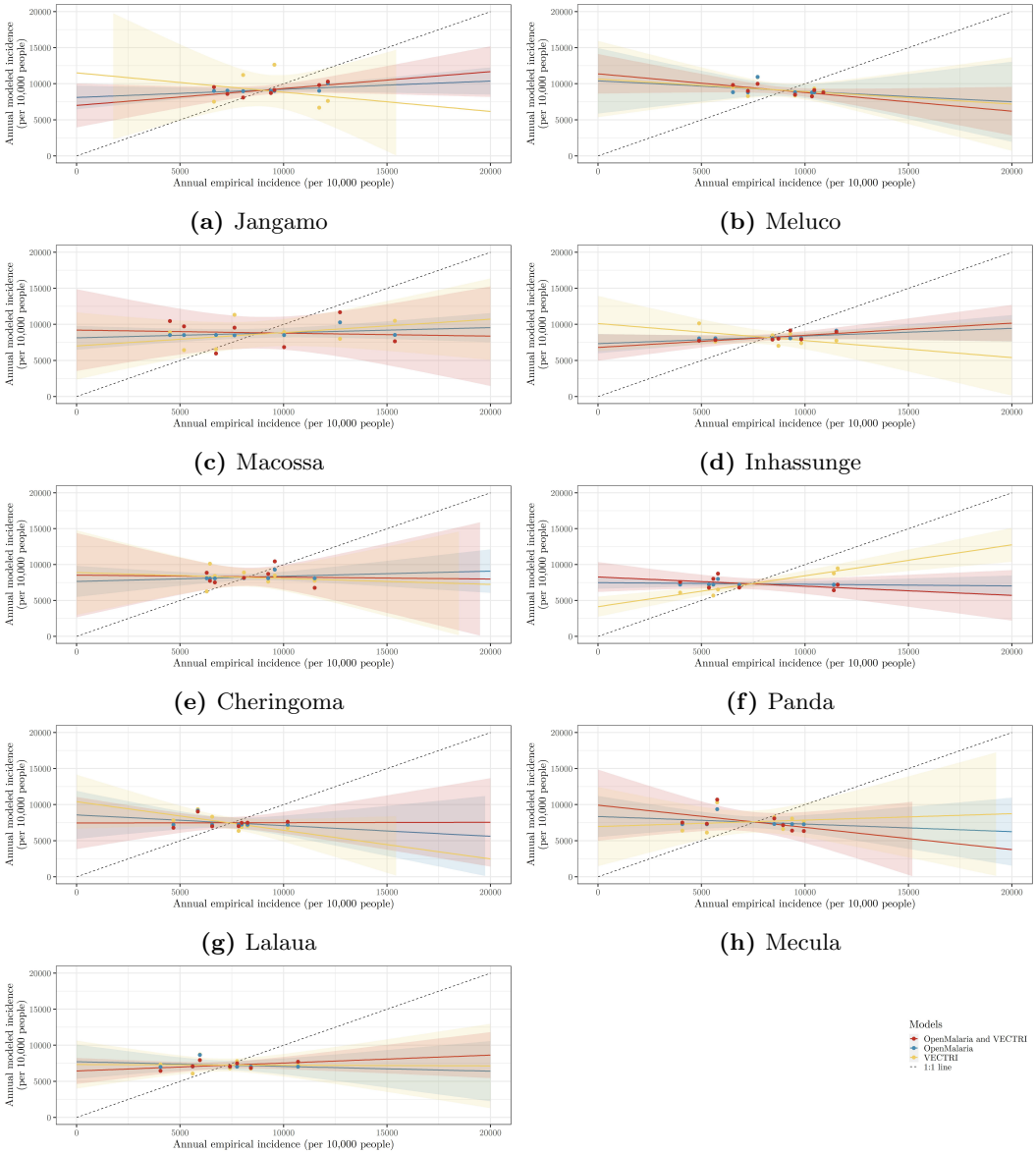

(a) Jangamo

(b) Meluco

(c) Macossa

(d) Inhassunge

(e) Cheringoma

(f) Panda

(g) Lalaua

(h) Mecula

(i) Mecufi

Figure 14: Comparison of the empirical and modeled annual malaria incidence, for the 9 Mozambican districts with the highest incidence after Chibabava (shown in the main article). Each dot represent a year and a model. The x-value is the empirical incidence that year, while the y-value is the predicted incidence for that year, according to the model. For each model, we have scaled the over-all-years modeled incidence to have the same mean as the over-all-years empirical incidence (i.e, we used the time series data from Figure 11). We plotted the 1:1 line for reference.

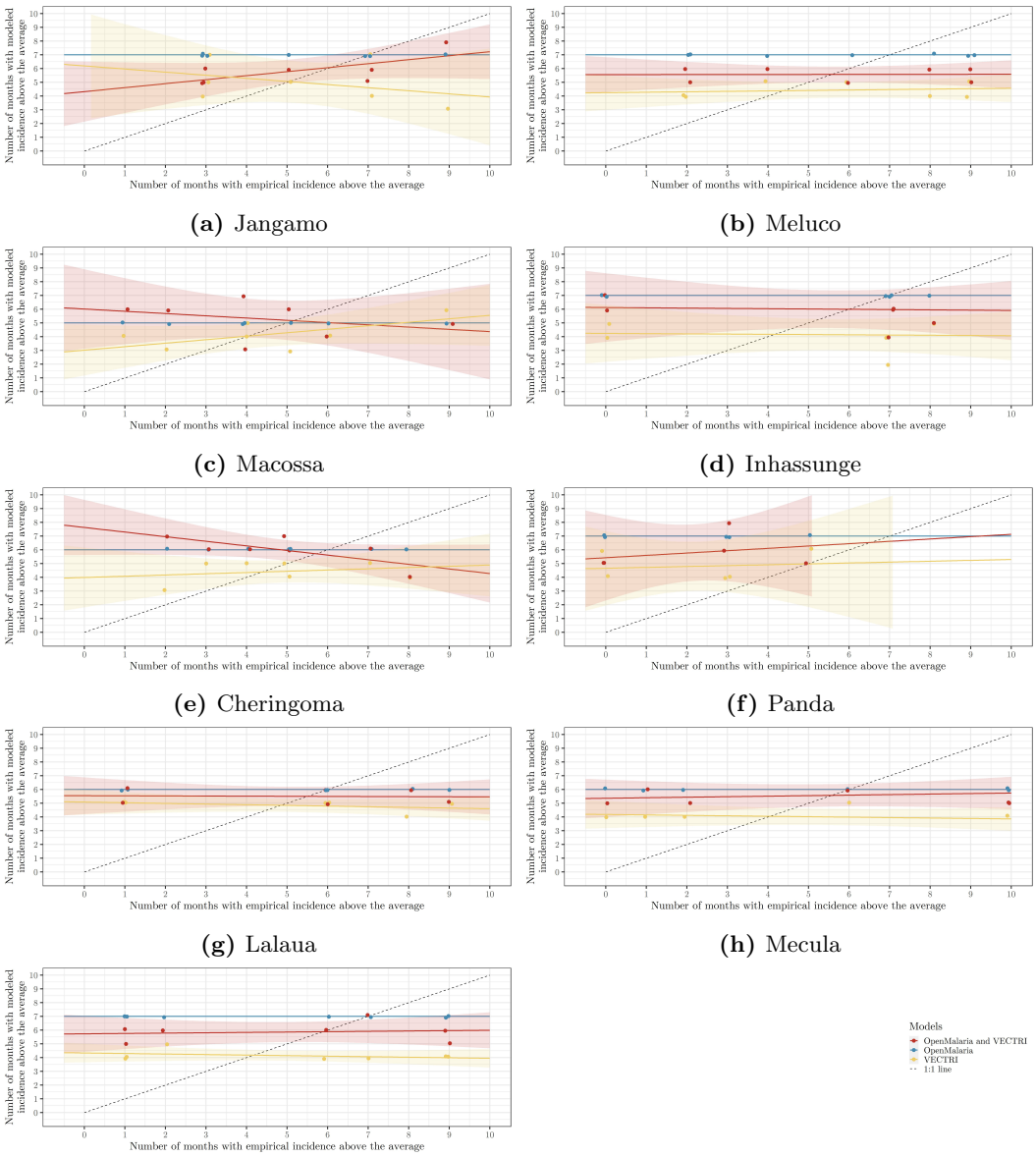

(a) Jangamo **(b)** Meluco **(c)** Macossa **(d)** Inhassunge **(e)** Cheringoma **(f)** Panda **(g)** Lalaua **(h)** Mecula **(i)** Mecufi

Figure 15: Comparison of the annual number of months with malaria incidence above the average, empirical against predicted by the models, for the 9 Mozambican districts with the highest incidence after Chibabava (shown in the main article). Each dot represent a year and a model. The x-value is the total number of months when the empirical malaria incidence that month was above the all-study-period average. The x-value is the total number of months when the predicted malaria incidence that month was above the all-study-period average, according to the model. For each model, we have scaled the overall modeled incidence to have the same mean as the overall empirical incidence (i.e, we used the time series data from Figure 11). We plotted the 1:1 line for reference.